GEOPHYSICAL INVESTIGATION FOR HYDROCARBON POTENTIAL OVER PART OF UPPER BENUE TROUGH (ADAMAWA BASIN) NORTHEAST, NIGERIA USING AEROMAGNETIC DATA

BY

AJALA, Sherifdeen Ayanniyi
M.Tech/SPS/2017/6850

DEPARTMENT OF PHYSICS
FEDERAL UNIVERSITY OF TECHNOLOGY
MINNA

SEPTEMBER, 2021

GEOPHYSICAL INVESTIGATION FOR HYDROCARBON POTENTIAL OVER PART OF UPPER BENUE TROUGH (ADAMAWA BASIN) NORTHEAST, NIGERIA USING AEROMAGNETIC DATA

BY

AJALA, Sherifdeen Ayanniyi
MTech/SPS/2017/6850

A THESIS SUBMITTED TO THE POSTGRADUATE SCHOOL FEDERAL UNIVERSITY OF TECHNOLOGY, MINNA NIGERIA IN PARTIAL FULFILLMENT OF THE REQUIREMENTS FOR THE AWARD OF THE DEGREE OF MASTER OF TECHNOLOGY IN PHYSICS (APPLIED GEOPHYSICS)

SEPTEMBER, 2021

ABSTRACT

This study present the results of the analysis and interpretation of aeromagnetic data over part of Adamawa trough with the aim of investigating the hydrocarbon potential of the study area. The study area covers an area of 12,000 km^2 located between latitude 8.50^{o}N and 9.50^{o}N and longitudes 11.50^{o}E and 12.50^{o}E. This study adopted both qualitative analysis and quantitative analysis to delineate the deep seated anomalies and estimate the sedimentary thickness for hydrocarbon maturation and accumulation respectively. Upward continuation and analytic signal techniques were used to delineate the deep seated structures using the total magnetic intensity map while three depth estimating techniques were employed to determine the thickness of sediments in the study area; Source parameter imaging, Euler deconvolution and spectral method. The analytic signal shows two major region; regions whose amplitude responses are high which are mainly basement intrusions with varying degree of deformations at the south-eastern to the central part the study area; and regions whose amplitude are low, which depicts regions with relatively good sedimentation at the northern part of the study area. The residual map was subjected to the depth estimating techniques and the results obtained corroborate; the SPI, Euler Deconvolution and Spectral method shows a thick sedimentation of 4.42 km, 4.20 km and 4.17 km at the north-eastern part of the study area respectively. The SPI, Euler deconvolution and the Spectral method reveal shallow depth of 0.06 km at the southeast, 0.10 km at the southeast and 0.42 km at the southwest part of the study area respectively. The maximum sedimentary thickness of above 4 km obtained in this study at the north-eastern part of the study area which corresponds to Numal is sufficient enough for hydrocarbon maturation and accumulation. The study area was found to have a good prospect for hydrocarbon exploration.

TABLE OF CONTENTS

LIST OF FIGURES

LIST OF TABLES

CHAPTER ONE

1.0 INTRODUCTION

1.1 Background of the Study

The substantial part of Nigeria source of income (80%) is acquired from hydrocarbon (oil and gas) profit whereupon more than 180 million teeming populaces depend (Adewumi *et al*., 2017). As the hydrocarbon potential of the prolific Niger delta becomes depleted or exhausted in the nearest future due to continuous exploitation and inherent crises in the existing oil producing region (Niger delta) which had led to undue reduction in oil production for export and domestic use, it is of necessity to shift attention to other inland sedimentary basins such as the study area (Adamawa Basin) in Nigeria for possible hydrocarbon exploitation.

The exploration for solid minerals, oil and gas across the Benue trough and its adjoining areas has increased tremendously with the aim of increasing the nation's hydrocarbon reserve and alternative means of generating more revenues. The interest in sedimentary basins arises from the fact that they are the usual potential host rocks for oil and gas and most solid minerals. The discovery and harnessing of hydrocarbon in the study area will expand Nigeria's oil and gas holdings, boost quantities of the hydrocarbon potentials of the Nigerian inland basins, in this way, help the economy of Nigeria and also provide many new employments to lessen unemployment rate currently facing Nigeria (Adewumi *et al*., 2017).

The present study attempts to use the qualitative and quantitative interpretation of aeromagnetic data over part of Adamawa Basin to examine the subsurface structures of the study area for possible hydrocarbon maturation and accumulation within the area using some advanced enhancement techniques.

Magnetic anomaly maps generally reflect variations in the Earth's magnetic field resulting from the underlying rocks' magnetic properties (e.g. magnetic susceptibilities). Though most rock-forming minerals have negligible to very low magnetic susceptibility and therefore are essentially non-magnetic, certain types of rocks contain enough magnetic minerals (especially magnetite) to generate recognisable magnetic anomalies. Sedimentary rocks generally have the lowest magnetic susceptibility, whereas metamorphic and basic igneous rocks have the highest magnetic susceptibilities (Dobrin and Savit, 1988; Telford *et al.*, 1998; Kearey *et al.*, 2002). Magnetic anomalies are caused by magnetic minerals contained in rocks; such anomalies are usually associated with underlying basement (igneous and/or metamorphic) rocks or by igneous bodies within sedimentary successions such as intrusive plugs, dykes, sills, lava flows and volcanic rocks (Gunn, 1997), as well as due to cultural iron contamination and heterogenic alterations in sedimentary rocks possibly caused by hydrocarbon migration (Costanzo-Alvarez *et al*., 2000; Aldana *et al*., 2003).

The magnetic method is useful whenever the object of investigation has a contrast in the magnetic susceptibility or remanence that can be detected by the magnetometer. This oldest of the geophysical exploration method is used for:

i. Location and definition of the extent of a Sedimentary Basin
ii. Depth determination to the basement rock (Magnetic source)
iii. Thickness of the sediment present which can be used to assess whether the sediment is enough to warrant exploration of petroleum.
iv. Local relief of the basement surface which may produce the structural relief in the overlying sediments.
v. Basement lineation

Analysing the local geology based on the deviations found in the earth magnetic field is the main aim of the magnetic survey of the earth subsurface. The magnetic surveying method uses the Earth magnetic anomalies ensuing from the magnetic properties of the underlying rocks to investigate subsurface geology. This anomaly mostly occurs as a result of the differences in the magnetic susceptibility of the rocks underlying subsurface.

Magnetic survey can be performed on Land, at Sea and in the air (as in the data to be used in this study), when performed in air an aeromagnetic study is undertaken and as such a magnetometer is towed behind an aircraft. The technique is widely employed and the speed of operation of airborne (Aeromagnetic) survey makes the method very attractive in the search for minerals and hydrocarbon explorations.

Aeromagnetic surveys have become common in hydrocarbon exploration in recent years. The development of more accurate magnetometer, aircraft positioning and data processing have led to the acquisition of high-resolution aeromagnetic surveys. Therefore, this work is an attempt to characterize geological structures and sedimentary basins in the Adamawa Trough and some adjoining areas by the use of potential field data.

Aeromagnetic data have long been used by the petroleum industry to map geological structures in, and to estimate depth to magnetic basement (Steenland, 1965). The computer processing and interpretation of the Aeromagnetic data led to anomaly estimation of depth to basement (Spector and Grant, 1970). The aeromagnetic survey is widely applied to the exploration for minerals and geothermal resources. This method was re-discovered by the petroleum industry in the early 1990s. It has been demonstrated in presentations, the literature and other forums that high resolution aeromagnetic data provide valuable data to solve petroleum exploration problems. High resolution aeromagnetic data for petroleum exploration are commonly defined as data collected at a flight line spacing of 800 metres or less, at flight-heights of 150 metres or less, at 15 metres or less sample spacing along the flight lines and at better than 0. I nT accuracy.

1.2 Statement of the Research Problem

Hydrocarbon is a major source of revenue in Nigeria. The substantial part of Nigeria's source of income (80%) is acquired from hydrocarbon (oil and gas) profit whereupon more than 180 million teeming populace depends on upon. The depleting nature of hydrocarbon potential of the prolific Niger Delta region stages a major concern and the activities of the militancy in the Niger delta calls for the need to delve into other inland sedimentary basins in Nigeria such as the Adamawa trough presumed to be rich in hydrocarbon. This study therefore attempts to analyses and interpret the high-resolution aeromagnetic data over the study area to assess its hydrocarbon potential.

1.3 Aim and Objectives of the Study

The aim of this study is to analyse and interpret aeromagnetic data of part of Upper Benue trough (Adamawa Basin) for possible hydrocarbon accumulation.

The objectives are to;

i. produce the composite map of the study area and interprets its total magnetic intensity (TMI) map
ii. delineate subsurface structures (long wavelength anomaly) in the study area using upward continuation filter and analytic signal.
iii. determine the sedimentary thickness using SPI, Euler deconvolution and spectral depth analysis
iv. delineate areas of possible hydrocarbon potential in the study area.

1.4 Justification of the Study

Benue trough is largely referred to as failed rift valley (Cratchley *et al.*, 1984 and Nwogbo, 1997) and so it is expected that the region should be a major depositional basin and therefore a good site for hydrocarbon maturation and accumulation.

With the availability of high-resolution aeromagnetic data, this study will properly contribute to the knowledge of the sedimentary thickness, which is one of the factors for possible accumulation of hydrocarbon within the study area.

1.5 Scope of Study

This work is limited to the analysis and geophysical interpretation of the four aeromagnetic data acquired for this research and to speculate on possible hydrocarbon potential within the area. This aeromagnetic study of Adamawa Trough is limited to the information that can be derived from the potential field.

1.6 The Location of the Study Area

This study covers an area of approximately 12,100 km^2 in the north-eastern part of Nigeria. The area (Figure 1.0) is bounded by latitudes 8.5 ^{0}00'N to 9.5^{0}00'N and longitudes 11.5^{0}00′E to 12.5^{0}00’E. The study area is located Adamawa Basin in the North Eastern part of Nigeria and covering Dong, Numal, Monkin and Jada.

The area has two distinct seasons; dry and wet. The dry season usually last from November to February and the rainy seasons last from March to October. Wet season starts normally from early April till ending of October, on average of about 210 days. While the dry season last from early November to March ending, on average of about 150 days. The first half of the dry season is called harmattan period (with night-time temperatures drop of as low as 11 °C) while the average monthly temperature for the dry season range from 21–25 °C.

The vegetation of the study area falls within the southern Guinea Savanna zone. The vegetation type is an open forest of tree savanna (mostly economic trees) where clusters of trees stands amongst grass and shrubs (Plateau and Nassarawa Geographical Information System).

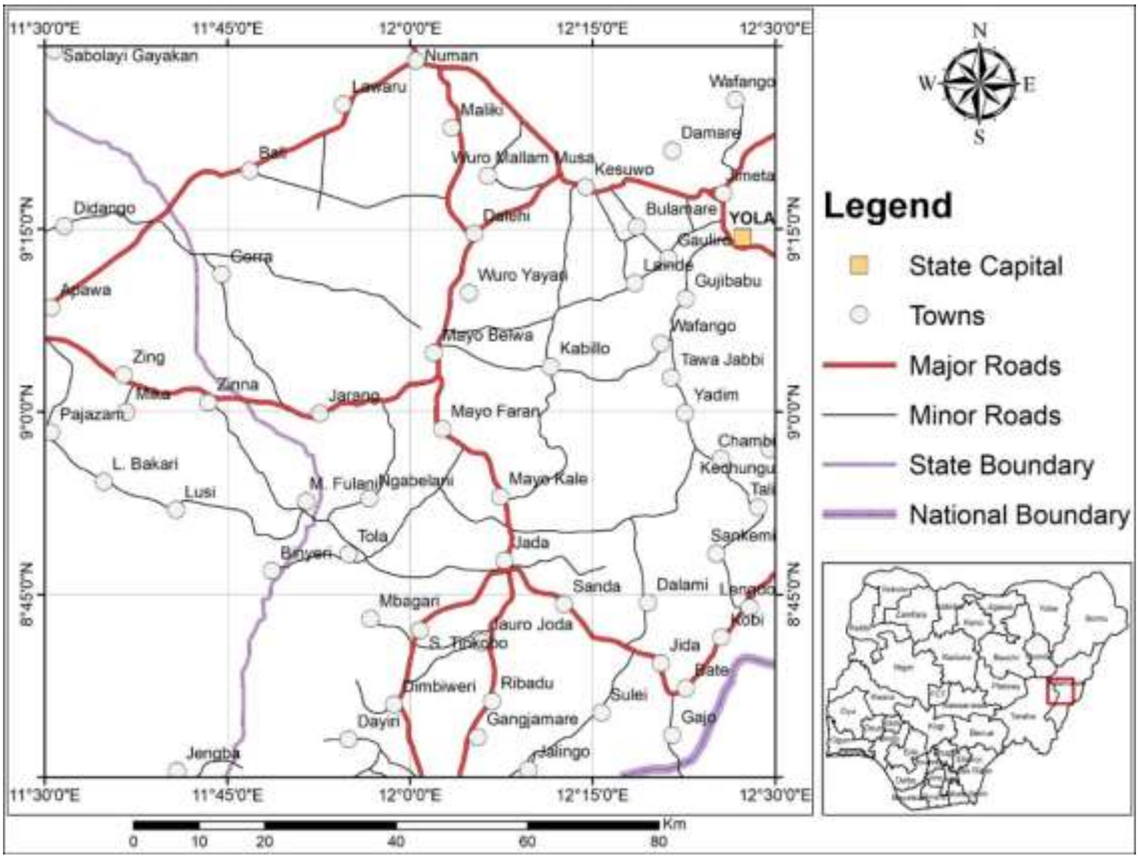

Figure 1.1: Location map of the study area

CHAPTER TWO

2.0 LITERATURE REVIEW

2.1 Geology of the Study Area

The study area is bounded by middle Benue trough. The Benue Trough formed during the Cretaceous as a result of the opening of the Atlantic Ocean. The Benue Trough (figure 2.0) in comprises of a progression of rift basins that model a portion of the Central West African Rift System of the Niger, Cameroon, Chad and Benin Basement fracture, subsidence, block faulting and cracking. It is an intercontinental basin of about 1000 km long and over a width of about 120 km from the northern parts of the Niger Delta Basin in the south west to the edges of the Chad Basin on the north east. The Nigeria Benue trough is boarded in the North West by Bauchi basement complex and the anorogenic granite of Jos plateau. Towards the South-West it is ended by the Precambrian gneisses, migmatites and rocks of the urban massifs of Calabar, while the southwest expansion of the trough was rapidly terminated by the more, younger sediment of the Niger-Delta. To the North-East the trough is ended with the underlying basement and the Biu volcanic (Nwachuku, 1972 and Ofoegbu, 1984).

On the structural feature of the Benue trough, the Benue trough is one of a kind among fracture valleys in that it is loaded with already folded sediments along North-East axis parallel to its length and its abnormal width which is three times that normally associated with rift valley (Ajayi and Ajakaiye, 1981). It structure is generally defined by folds formed in the Cenomanian (Nwachuku, 1972) and Santonian, (Orajaka, 1972 and Olade, 1975). The Benue Trough earlier (Albian-Santonian) sediments are mainly marine in character and their deposition was terminated by a late episode of deformation in the Santonian Burke *et al* (1970). The silt is made up of sandstones, shales and limestone and dominated by Precambrian basement (granites and gneisses). The prior (Albian–Santonian) silts in the trough are primarily marine in character and their disposition was ended as a result of deformation in the Santonian. Subsequently after this deformity the marine silt were dissolved and deltaic sediments spread all through the trough. (Cater *et al.*, 1963 and Fitton, 1980).

Benkhelil (1982 and 1989), described the Benue Trough as a set of juxtaposed pull –apart basins generated along pre-existing N60^{0}E strike–slip faults during the early Cretaceous. It is geographically and structurally subdivided into three parts erroneously termed as "lower Benue Trough", "middle Benue Trough" and an "Upper Benue Trough".

The Benue trough which specifically housed the study area belongs to the genetically and physically related systems of faults and rifts referred to as the West and Central African Rift System (Alagbe and Sunmonu, 2014). The system’s origin is attributed to the breakup of Gondwanaland and the opening of South Atlantic and Indian Ocean. The Upper Benue – Chad axial trough is believe to be the third and failed arm of a triple junction rift system that preceded the opening of the South Atlantic during the early Cretaceous and subsequent separation of African and South American continent (Adegoke, 2012).The essential geological features in the basin (Fig. 1) consist of sedimentary rocks ranging in age from upper Cretaceous to Quaternary, overlying an ancient crystalline basement made up mainly of Precambrian granites and gneiss. The Cretaceous sediments and the underlying basement complex, as in most other parts of Nigeria, are invaded by numerous minor and major intrusions of intermediate to basic composition. The older intrusive are largely granites and granodiorites while the younger intrusive are mainly granitic and pegmatitic types, although diorites and some synetites also occur. There were also occurrences of igneous and volcanic activities within the region extending from cretaceous to recent times. Prominent among the Tertiary and Recent volcanic in the region are the basic lavas of Biu and Longuda. The crystalline basement whose topography is believed to be irregular (Carter *et al.*, 1963) is exposed in a number of locations in the region. Intruded into the basement is a series of basic, intermediate and acid plutonic rocks referred to as the older Granites. Notable outcrops of the older Granites include the small inliers of biotite granites which are found around Kaltungo, Gombe, Kokuwa, and in the Bauchi area. The uplifted basement rocks in the North-westen part of the area were also intruded by orogenic acid ring complexes, the Younger Granites (Alagbe and Sunmonu, 2014 and Ajakaiye *et al.,* 1985). Numerous faults have also been reported in the region (Ajakaiye *et al.,* 1986). These faults show variable trends but the dominant direction lies between NNE and ENE (Alagbe and Sunmonu, 2014).

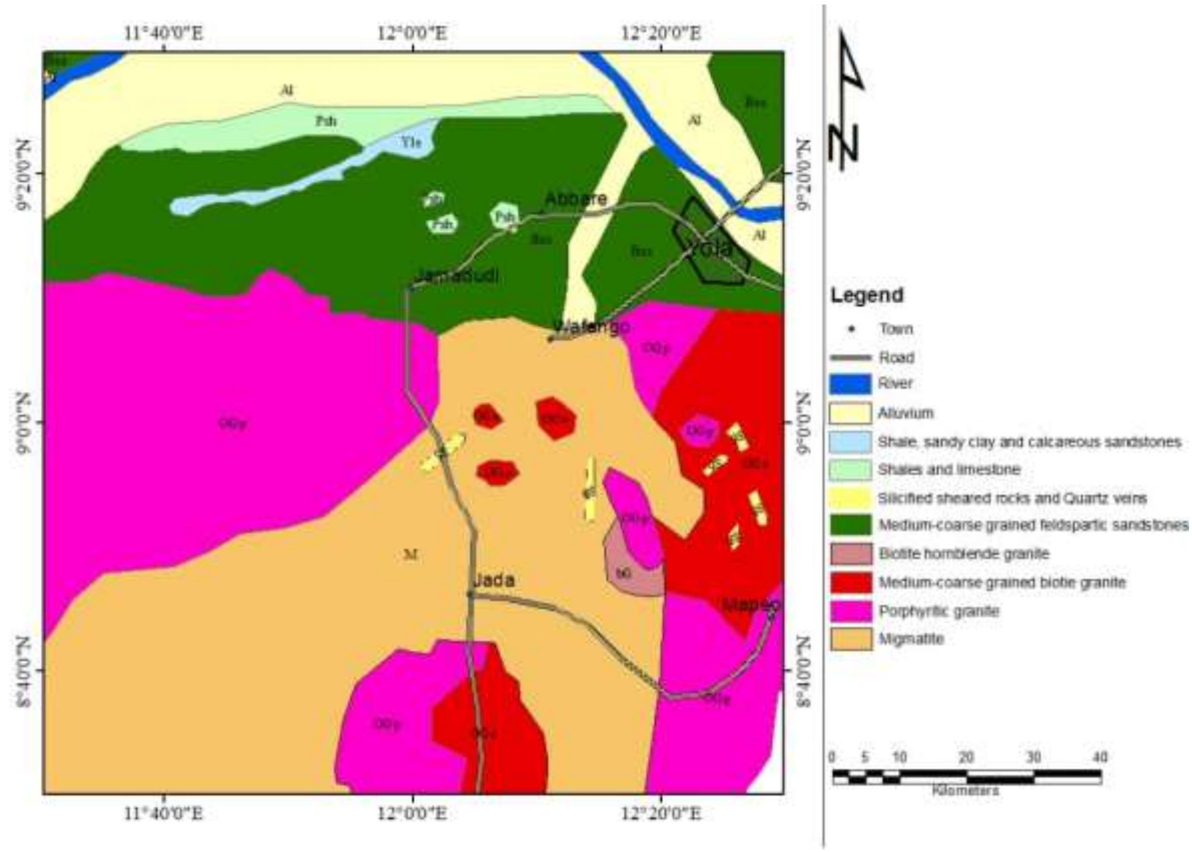

Figure 2.1: Geological map of the study area

2.2 Review of Previous Geological Studies

However, there has been more extensive and intensity geological activity in the Trough with renewed attempts at more detailed geophysical studies in the past years. This has led not only to a better understanding of the structure of the Benue Trough, but also its origin and evolution. In terms of tectonic evolution of the Benue Trough, Nwachukwu (1972) studied it in term of marine transgression and regression. He listed some tectonic successions of the Trough. These include the Albian transgression followed by the Cenomanian regression, Turonian transgression that was followed Coniacian and Maastrichtian. The Basin narrows towards the East and disappears under the Tertiary and Recent rock from the Cameroon volcanic axis containing basalt, trachyte and ryholic (Fitton,1980)

Olade 1975 indicated that the tectonic evolution of the Benue trough comprises of the rise of mantle upwelling or plume positioning of intrusive igneous rock in the crust, stretching, diminishing and consequently rifting of the crust as he used tectonic model to carry out research on the evolution of the trough.

Offodile (1976) had illustrated that Benue Trough has recognizable conditions for the beginning and aggregation of hydrocarbons in oil bearing trap in light of the fact that oil source rocks are created in a marine depreciation condition and the reservoirs have adequate permeable sandstones of 'Gombe series'.

Haruna *et al.*(2012), Le Roux (1991) and Suh *et al*. (2000) have all demonstrated that upper parts of Benue trough have deposits of Uranium bearing sandstone with momentous contributions from Lacustrine Delta deposits, they reported that background radiometric reading for the numerous facies of this Uranium bearing sandstone vary between 90 cps to 250 cps. They concluded that certainly the variations surely not inconsistent to the changing sedimentological components of the various Bima members. Le Roux (1993) suggest that the permeability of this kind of deposits must not be excessively important in light of the fact that a too high permeability leave short time for Uranium to accelerate from Ore bearing fluids

2.3 Review of Previous Geophysical Studies

Ajakaiye, 1981 and Ofoegbu, 1984 by their analysis of both ground and airborne magnetic data over the Benue Trough have shown extensive block faulting in the trough. These faults in places attain considerable lengths and mark out several basinal structures in the trough. Examples include the Anambra basin, Afikpo basin etc.

Both magnetic survey and gravity survey done to estimate the sedimentary thickness of the arrives at approximate same result, Osazua *et al.* (1981) using gravity method computed the thickness of sediments in the Yola portion of the upper Benue trough to range from 0.9km to 4.9 km while Ofoegbu (1988) using magnetic method computed the sediment thickness of the same region to range from 0.5km to 4.6km. The later stated that although the anomalies over the Upper Benue Trough can be separately accounted for in terms of basement variable topography or intrusive bodies, they were best interpreted in terms of the combined impacts of crystalline basement of variable topography and intrusive bodies.

Onuoha *et al.* (1994) carried out two-dimensional spectral analysis of Aeromagnetic data over the middle Benue Trough in order to estimates average to magnetic source in the area. Their result indicates two depth source model with depth to deeper source varying between 1.6 km to 5 km while that of shallower source vary in between 0.06 km to 1.2 km.

Nwogbo (1997) in order to estimate location of magnetic source mapped shallow source in the upper Benue trough using spectral analysis and He established that the mean depth basement varies between 2 km to 2.62 km which conforms to the region fine topography. Mean depth to the shallow source ranges from 0.07 km to 0.63 km which he said may be associated to either shallow intrusive bodies or some close surface basement. He noted that there are few deeper intrusive at 2.45 km within the basement.

Chinwuko *et al.* (2012) Carried out detailed interpretation of the aeromagnetic data over parts of Upper Benue Trough and Southern Chad Basin. They model prominent magnetic anomaly and also determine various temperatures at depth in the study area. Two depth source models were interpreted using Discrete Fourier Transform method. They reported depth to the deeper magnetic sources to vary between 1.5 km and 2.5 km and the depth to the shallower magnetic source to ranges from 0.5 km to 1.4 km. They concluded that based on the sedimentary thickness of 1.5 km to 2.5 km and the temperature at depth of 81^0C-115^0C, the possibility of hydrocarbon generation towards the northeastern part of the study area is feasible.

Okonkwo *et al.* (2012) carried out Interpretation of Aeromagnetic data over Maiduguri and Environs of Southern Chad Basin of the upper Benue trough, they established that **d**epth to the basement of the basin structure ranges from about 0.5 km in the southern part of the study area and gets deeper toward the northern part up to 3.0 km. they noted that the trend system of the area is approximately NE-SW direction and subordinate W-E direction and that this trend conforms to the trend of the Basin itself. They concluded that the depth to basement map of the study area shows clearly that the sedimentary cover is generally shallow towards the western parts and therefore is not likely to favour hydrocarbon formation. But at the eastern parts, the map showed thick sedimentary cover which may favour hydrocarbon when all other conditions necessary for hydrocarbon formation are present.

Salako and Udensi (2013) carried out spectral analysis of part of upper Benue trough in order to established sedimentary thickness beneath the surface in the area. From the result of their study they established two layers with the first layer depth ranges between 0.268 km to1.08 km with maximum depth at the north central part and the minimum depth at south eastern and south western part; they attributed this first layer depth to the magnetic rocks that intrude the sedimentary formation, While the second layer thickness ranges from 2.06 km to3.35 km with highest of 3.35 km attained at the northern part of the area which corresponds to Damaturu and Bulkachuwa area. Muhammed and Mustapha (2014) in order to evaluate magnetic basement depth over parts of Bajoga and environs of part of upper Benue trough estimated the magnetic residual anomaly of high value of +116nT for Malleri and Dukul portion and low values of about -134 nT for Bajoga and Bage portion.

Nwosu (2014) used source parameter imaging of aeromagnetic data to estimate depth to Magnetic Basement over Parts of Middle Benue Trough, he established a two layer depth model and predominant NE-SW lineament trend, his shallower magnetic source has an average depth of 1079.5 m while the deeper magnetic source bodies have an average depth of 3245 m.

Abdullah *et al.* (2014) investigate the magnetic exploration of the upper and lower part of the Benue trough for metallic deposits and hydrocarbon. They found the depth to intrusive to range 3.2 km and 3.9 km and depth to deep structure range from 8.7 to 9.2 km. They concluded that most of the intrusive are dyke shape which they suggested that the intrusive might contains Rholerite, Basalt Granite and Dolerite.

Alagbe and Sunmonu (2014), carried out an Interpretation of Aeromagnetic Data from Upper Benue Basin Using Automated techniques involving the analytic signal, horizontal gradient magnitude and the log power spectrum techniques to delineate linear geologic structures such as faults, contacts, joints and fractures in the area. Results from their analytic signal technique showed that the basement in the area is segmented by faults whose depth ranges between 0.5 km and 10.5 km with an overall average depth ranging from 1.13 km to 5.88 km.

2.4 Rock Magnetic Properties

In every case, the susceptibility (K) of rocks depends on the amount of magnetite (Fe_30_4) contained in the rock unit. K is the significant variable in magnetic playing the same role as density in gravity exploration. Magnetic susceptibility, property is represented as a range even for a particular rock and a wide overlap between rock types. The magnetic susceptibility is measured either in nanotesla or gamma (γ) values. Table 1.1, below shows the magnetic susceptibilities of some basic rocks

Aeromagnetic maps represent magnetic-field variations caused by differences in the total magnetisation of underlying sources. Total magnetisation is the vector sum of induced and Remnant components.

Table 2.1: Typical Magnetic Susceptibilities of Earth Materials. (Dobrin, 1986).

Rock (Mineral)	Type Susceptibility (c.g.s.)
Magnetite	0.3 -0.8
Pyrrhotite	0.028
Ilmenite	0.044
Specularite	0.004
Iron Formation	0.056
Basalt	0.00295
Diabase	0.00259
Rhyolite	0.00112
Gabbro	0.00099
Granite	0.00047
Other Acid Intrusive	0.00035
Ely Greenstone	0.00009
Slates	0.00005
Sedimentary Rocks	0.00001 to 0.001

The induced component of a rock is the product between the Earth's present-day magnetic field vector and the magnetic susceptibility. Magnetic susceptibility is a scalar measure of the quantity and type of magnetic minerals (commonly titanomagnetites) in the rock. The remnant component (also a vector) is based on the permanent alignment of magnetic domains within magnetic minerals and is measured using Paleomagnetic methods (Butler, 1992).

Igneous and crystalline metamorphic rocks commonly have higher total magnetisations compared to other rock types, whereas sedimentary rocks and poorly consolidated sediments have much lower magnetisations (Reynolds, 2011). Total magnetisations of volcanic rocks are normally dominated by the remnant component, whereas those for all other rock types are dominated by the induced component, with the exception of some mafic metamorphic rocks (Reynolds, 2011). Aeromagnetic anomalies over volcanic rocks commonly produce high-amplitude positive or negative anomalies. Where a correspondence between volcanic edifices and anomaly shape can be demonstrated, positive and negative anomalies indicate normal and reversed-polarity remnant polarities of the rocks respectively. Theoretically, the magnetic methods are based on the measurement of the small variation in the distribution of the magnetised or polarised rocks.

A sedimentary basin is a depression that has accumulated sediment from the basement rocks. If it contains numerous magnetic rocks such as igneous intrusions or extrusive, magnetic sediments or magnetic metamorphic units, these can provide information on the morphology of the sedimentary basin and its structure. However, if the magnetic units in the basement occur at the basement surface, then the depth determinations for these will map the basin floor morphology. This approach has been used for several decades to locate sedimentary basins with significant thicknesses of sediment (Milligan and Gunn, 1997). Depth to basement, faults in the basement surface and relief of the basement have direct relevance to the depositional and structural history of a basin. Many examples exist of positive basement block being directly related to depositional isopaches and / or structure which reflect the underlying basement structure. In general, igneous rocks have higher content of magnetic minerals especially magnetite than sedimentary rocks and can be identified and mapped in the sedimentary basin from the magnetic data. Igneous features such as intrusive plugs, dykes, sills, lava flows and volcanic centres can occur at any stage of a basin’s evolution and therefore be preserved at any level in the sedimentary section. Such features are significant in understanding the history of a basin and assessing its petroleum or mineral prospectively. Igneous intrusions can produce structural closure and here, magnetic anomalies can be indicators of hydrocarbon traps.

In sedimentary sections, magnetic anomalies caused by non – igneous sources with sediments, are typically weaker than those due to the basement and metamorphic rocks which generally contain much greater concentrations of the magnetic minerals. Sedimentary layer may be magnetic if they contain enough magnetic minerals. However, they must have structural relief for them to give rise to a magnetic anomaly. Magnetic sheets only have anomalies at the edges. Small concentrations of magnetite in sediment can produce an observable magnetic response. However, in sedimentary environments, detrital is rapidly oxidized to hematite which is marked less magnetic, although hematite can in sufficient concentration produce an observable magnetic effect. Magnetic anomalies may be caused by disseminated pyrrhortite in shale and siltstone. Ilmenite may give also a weak magnetic response and ancient beaches are known to contain enough of this mineral to give a weak observable response (Mudge, 1994)

Nevertheless, pure salt comprising halite, gypsum and anhydrite is diamagnetic as such it has a negative magnetic susceptibility and as a result normally has a negative magnetic contrast relative to enclosing sediments. In such situation, high sensitivity magnetic survey map salt dome and salt ridge as magnetic lows.

CHAPTER THREE

3.0 MATERIAL AND METHODS

3.1 Materials

The materials used for this study includes the following

i. Aeromagnetic data covering the study area
ii. Oasis Montaj Software v8.4
iii. Microsoft Office (Word and Excel Packages)
iv. Laptop (work station)
v. Surfer 13 software

3.1.1 Aeromagnetic data acquisition

For this research work, four aeromagnetic data sheets in half by half degree (55 x 55 sq.km) used were procured from the Nigerian Geological Survey Agency (NGSA) Abuja. The data was collected as a part of the nation aeromagnetic survey carried out in 2009 by Fugro Airborne survey. The four aeromagnetic data sheets acquired are 195 (Dong), 196 (Numal), 216 (Monkin) and 217 (Jada) which correspond to area covered by latitude 8.5^0N to 9.5^0N and longitude 11.5^0E to 12.5^0E. Below are the technical details of the survey/ flight parameters:

Flight line spacing: 500 m

Terrain clearance: 100 m (Ogun state), 80 m (Phases I and II)

Flight direction: NW - SE

Tie lines spacing: 2 km

Tie lines direction: NE -

3.2 Methodology

3.2.1 Data analysis

The first step in this work is to assemble and knit the acquired data which is in separate sheets to produce the Total magnetic intensity (TMI) map of the study area. The next step is to perform regional/residual separation on the TMI map of the study area.

The residual map will then be subjected to the following methods to estimate the sedimentary thickness of the study area for hydrocarbon maturation;

i. Spectral analysis

ii. Source parameter imaging

iii. Euler deconvolution

3.2.2 Production of Total Magnetic Intensity (TMI) Map

The four total field aeromagnetic sheets will be assembled, merge, and transported into Oasiss montaj 8.4 v software to produce the map of the total magnetic intensity (TMI). The Oasis montaj software is primarily designed for potential data analyses, which uses Fourier domain techniques for data transformation.

3.3 Data filtering

3.3.1 Regional and residual separation

The Total Magnetic Intensity and even the aeromagnetic field sheet used in producing it are the entirety of the effect of all sources generating the magnetic anomaly. In applied geophysics, the issue is to dispose with or lessen to a minimum, the impacts of deep seated, non-profitable sources with minimum disturbance of the resultant anomaly as could reasonably be expected.

The Regional-Residual separation involves a careful analysis of the potential field profile in the area within and beyond the area of immediate concern the map.

Thus, this work (interpretation of the magnetic field) begins with the separation of the long-wavelength anomalies of the regional field component which is attributed to deep and large scale sources from the shorter wavelength features constituting the residual field assumed to arise from shallow, small scale sources.

Theory of Methods

3.3.2 Upward continuation of the potential Field

Continuation methods project the observed potential (gravity and magnetic) anomaly field to higher elevations (upward continuation) or lower elevations (downward continuation) and therefore, effectively serve as low-pass and high-pass filters respectively (Khalil 2012)

Upward continuation is a filter operation, which smoothens the original data by attenuation of short wavelength anomalies relative to their long wavelength counterparts. In the space, the upward continuation operation is a two dimensional convolution process given by the integral equation (Bhattacharyya, 1975).

$$\phi'(x,y) = \int_{-\infty}^{\infty}\int_{-\infty}^{\infty} f(\alpha,\beta)\phi(x-\alpha, y-\beta)\,d\alpha d\beta \qquad (3.1)$$

Ø´(x,y) is the input data, Ø(x,y) is the output data and f(α,β) is the filtering function.

In order that a filtering function can be useful, it must be of finite extent, if f(x,y) becomes zero for |x|=|X| and |y|=|Y| then equation (3.1) can be replaced by

$$\phi'(x,y) = \int_{-X}^{X}\int_{-Y}^{Y} f(\alpha,\beta)\phi(x-\alpha, y-\beta)\,d\alpha d\beta \qquad (3.2)$$

Convolution in the space domain is equivalent to multiplication in the frequency domain. In order to arrive at the spectrum of the output, the spectrum input is multiplied by the spectrum of the filtering function. Denoting the Fourier transform of a function by the corresponding capital letter, with a frequency argument and taking the Fourier transform of Equation (3.2). Thus we have:

$Ø\,'(f_x,f_y) = F(f_x,f_y)\,Ø(f_x,f_y)$ (3.3)

Where f_x and f_y are the angular frequencies along x and y axes respectively, From the results of the potential theory, the upward continuation of the potential function Ø(x,y,0) in a source free region to a height(h) above the plane Z=0 is given by (Hahn,1976)

$$\phi'(x,y,h) = \int_{-\infty}^{\infty}\int_{-\infty}^{\infty}\frac{h\phi(\alpha,\beta,0)\,d\alpha d\beta}{2\pi\sqrt{[(x-\alpha)^2+(y-\beta)^2+h^2]^3}} \qquad (3.4)$$

Comparing equation (3.4) and (3.1), and realizing that the convolution integral is commutation, allows recognition of equation (3.4) as a two dimensional convolution and hence a filtering operation. The potential function Ø(x, y, 0) is operated upon by the filtering function f_u (x,y,h) in order to arrive at Ø(x,y,h) where

$$f_u(x,y,h) = \frac{h}{2\pi\sqrt{(x^2-y^2+h^2)^3}} \qquad (3.5)$$

The theoretical frequency response of a true upward continuation operator may be obtained by the Fourier transform of equation (3.5) or the solution of the integral

$$f_u(f_x,f_y,h) = \int_{-\infty}^{\infty}\int_{-\infty}^{\infty}\frac{he^{-2\pi i(f_x x+f_y y)}}{2\pi\sqrt{(x^2+y^2+h^2)^3}}\,dxdy \qquad (3.6)$$

Solution of this equation by gamma functions (Fuller,1967) yields

$$F_u(f_x, f_y, h) = e^{-2\pi h\sqrt{(f_x^2+f_y^2)}} \tag{3.7}$$

Equation (3.7) describes the desired frequency response of an upward continuation operator.

3.3.3 Analytic signal

The analytical signal method is very important to this research by which it suggests the location of magnetic source is coming from. Analytical Signal Method: (Nabighian1972, 1974) developed the concept of two-dimensional analytical signal, or energy envelope of magnetic anomalies. Roest *et al.* (1992) Showed that the amplitude of the three dimensional analytical signal at location (x,y,z) can be expressed as

$$|A(x, y,)| = \sqrt{(\frac{\partial \mathrm{M}}{\partial \mathrm{x}})^2 + (\frac{\partial \mathrm{M}}{\partial \mathrm{y}})^2 + (\frac{\partial \mathrm{M}}{\partial \mathrm{z}})^2} \tag{3.8}$$

where,

$A\ (x, y)$ = amplitude of the analytic signal at (x, y),

M = observed magnetic field at (x, y).

The analytic signal is not dependent of magnetisation direction and Earth's magnetic field direction. This implies that all bodies with similar geometry have the same analytical signal (Milligan and Gunn, 1997).

3.4 Depth Analysis

Depth to basement is important in our exploration efforts, particularly for the determination of depths in areas where there maybe mature hydrocarbons. Reliable depths help drilling plan for both magnetic and non-magnetic targets.

The methods employed in the analysis of depth are analytic signal, source parameter imaging and spectral analytical method.

3.4.1 Source parameter imaging (SPI^{TM})

The Source Parameter Imaging (SPI^{TM}) is a technique using an extension of the complex analytical signal to evaluate magnetic depths. The Source Parameter Imaging TM (SPI^{TM}) function is a fast, simple, and capable method for computing the depth of magnetic sources. Its accuracy has been demonstrated to be +/- 20% in tests on real data sets with drill hole control. This accuracy is analogous to that of Euler deconvolution, however SPI has the advantage of delivering a more complete set of coherent solution points and it is easier to use (Salako 2014). One merit of the SPI technique is that the depth can be visualised in a raster format and the true thickness can be determined for each anomaly.

This approach developed by Thurston and Smith (1997) and Thurston *et al*. (1998) sometimes referred to as the local wave number method uses the connection between source depth and the local wave number (k) of the observed field, which can be calculated for any point within a grid of data through vertical and horizontal gradients (Thurston and Smith, 1997). The depth is shown as an image. The basics are that for vertical contact, the peaks of the local wave number define the inverse of depth.

The SPI method (Thurston and Smith, 1997) estimates the depth parameter using the local wave number of the analytical signal (Salako, 2014). The analytical signal $A_1(x, z)$ is defined by Nabighian (1972) as

$$A_1(x,z) = \frac{\partial \mathrm{M(x,z)}}{\partial \mathrm{x}} - \mathrm{j}\frac{\partial \mathrm{M(x,z)}}{\partial \mathrm{z}} \tag{3.9}$$

where; $A_1(x,z)$ = analytic signal

M(x,z) = magnitude of the anomalous total magnetic field, j = imaginary number, z and x indicate the gradients in the vertical and horizontal direction Also, Nabighian (1972) has demonstrated that the gradient changes constitutes the imaginary and real parts of the 2D analytical signal which are related as follows:

$$\frac{\partial \mathrm{M(x,z)}}{\partial \mathrm{x}} \Leftrightarrow -\mathrm{j}\frac{\partial \mathrm{M(x,z)}}{\partial \mathrm{z}} \tag{3.10}$$

where

⇔ implies a Hilbert transform.

Thurston and Smith (1972) defined the local wave number κ1 to be:

$$k_1 = \frac{\partial}{\partial \mathrm{x}} \tan^{-1}\left[\frac{\partial \mathrm{M}}{\partial \mathrm{z}} \Big/ \frac{\partial \mathrm{M}}{\partial \mathrm{x}}\right] \tag{3.11}$$

Salako (2014) and Nwosu (2014) illustrated that the signatures illustrated by Thurston and Smith (1972) utilised Hilbert transformation pair stated in (3.16). The Hilbert transform and the vertical derivative operators are linear, so the vertical derivative of (3.16) will give the Hilbert transform pair as

$$\frac{\partial^2 \mathrm{M(x,z)}}{\partial \mathrm{z}\, \partial \mathrm{x}} \Leftrightarrow -\frac{\partial^2 \mathrm{M(x,z)}}{\partial^2 \mathrm{z}} \tag{3.12}$$

Thus the analytic signal could be defined based on second-order derivatives, $A_2(x,z)$, where

$$A_2(x,z) = \frac{\partial^2 \mathrm{M(x,z)}}{\partial \mathrm{z}\, \partial \mathrm{x}} - \mathrm{j}\frac{\partial^2 \mathrm{M(x,z)}}{\partial^2 \mathrm{z}} \tag{3.13}$$

This gives rise to a second order local wave number K_2 , where

$$k_2 = \frac{\partial}{\partial \mathrm{x}} \tan^{-1}\left[\frac{\partial^2 \mathrm{M}}{\partial^2 \mathrm{z}} \Big/ \frac{\partial^2 \mathrm{M}}{\partial \mathrm{z}\, \partial \mathrm{x}}\right] \tag{3.14}$$

This first and second – order local wave numbers are used to determine the most appropriate model and depth estimate of any assumption about a model. In this study, the

SPI will be used to determine the thickness of sediment for hydrocarbon potential of the study area.

3.4.2 Spectral depth analysis

It is a depth estimating method used in geophysics. it is used in investigating the thermal frame work via aeromagnetic studies. Spectral depth analysis based on statistical models has been employed in numerous geophysical works, as in the determination of average depth to the top of magnetic basement and in the computation of crustal thickness.

The technique permits an estimate of depth of magnetised blocks of varying depth, width, thickness and magnetisation. Most approaches used include Fourier transformation of the aeromagnetic data to estimate the energy (or amplitude) spectrum. The Discrete Fourier Transform is the mathematical tool for spectral analysis and applied to regularly spaced data such as the aeromagnetic data. The Fourier Transform represented mathematically in as:

$$\mathrm{Y}_n(\mathrm{x}) = \frac{a_0}{2} + \sum_{n=1}^{N} \left(a_n \cos\frac{n\omega x}{L} + b_n \sin\frac{n\omega x}{L} \right)$$

(3.15)

where

L= dimensions of the block or map,

$Y_n(x)$ = reading at x_n position,

n = harmonic number at the number of data points,

a_n =real part of the Fourier amplitude,

b_n = imaginary part of the Fourier amplitude,

N= number of grid points along the horizontal and vertical components

ω = fundamental angular frequency and is given by $\omega = 2\pi / \sum x$,

$\sum x$ = the total length of x over which y(x) has been measured.

$a_n = \frac{2}{x}\int_{-x/2}^{x/2} y(x)\cos n\omega x \, dx$and

$$b_n = \frac{2}{x}\int_{-x/2}^{x/2} y(x)\sin n\omega x \, dx$$

The energy spectrum is then plotted on the Logarithmic scale against frequency. The plot shows the straight-line graph which diminish in slope with rising frequency. The slopes of the segments yield estimates of depths to magnetic sources.

Spector and Grant (1970) used the idea of an ensemble of prism to be statistical model for representing the target magnetic sources within any area. An ensemble is a collection of prisms whose parameters (width, length, thickness, body centre location) fluctuate over some extents and subsequently shapes a volume in the n-dimensional parameter space with each point in the volume relating to a particular prism.

If h is the mean depth of a layer and the depth factor for an ensemble hence, a plot of the energy spectrum of a single ensemble of prism against angular frequency r would yield a straight line graph whose slope is directly proportional to the average source depth, h of that ensemble. That is, the logarithm plot of the radial would yield a straight line whose slope,

$$m = -2h$$

$$h = -\frac{m}{2} \tag{3.16}$$

Equation (3.22) can be specifically applied if the frequency unit is in radian per unit distance (kilometer as it is in this research), if it is unit is in cycle per unit distance as it is in this work, the expression becomes

$$h = -\frac{m}{4\pi} \tag{3.17}$$

The sedimentary thickness of the study area will also be estimated from the spectral analysis of the aeromagnetic data of the study area.

3.4.3 Euler deconvolution

Euler deconvolution is a method to estimate the depth of subsurface magnetic anomalies and can be applied to any homogeneous field, such as the analytical signal of magnetic data. It is particularly good at delineating the subsurface contacts. It has been observed that the depth estimates from magnetic data are more accurate if the pole-reduced magnetic field is used, than when using the magnetic data themselves. Euler deconvolution was originally developed in exploration geophysics for rapidly estimating the location of and depth to magnetic or gravity sources. It is based on the fact that the potential field produced by many simple sources obeys Euler's homogeneity equation (Hood, 1965). If a given component of the magnetic anomalous field $\Delta T(x, y, z)$ satisfies the following equation:

$$\Delta T(x, y, z) = \mathrm{tn}\, \Delta T(x, y, z) \tag{3.18}$$

where n is the degree of homogeneity, then differentiating Equation 4 with respect to t gives Equation 5:

$$\mathrm{x}\frac{\partial \Delta T}{\partial \mathrm{x}} + \mathrm{y}\frac{\partial \Delta T}{\partial \mathrm{y}} + \mathrm{z}\frac{\partial \Delta T}{\partial \mathrm{z}} = \mathrm{n}\Delta T \tag{3.19}$$

where x, y, and z are the coordinates of the field observation points and assumed to be at the origin.

According to Thompson,, (1982), Considering the potential field data, Euler's deconvolution equation can be expressed as

$$(\mathrm{x}-\mathrm{x}_0)\frac{\partial \Delta T}{\partial \mathrm{x}}+(\mathrm{y}-\mathrm{y}_0)\frac{\partial \Delta T}{\partial \mathrm{y}}+(\mathrm{z}-\mathrm{z}_0)\frac{\partial \Delta T}{\partial \mathrm{z}}=\mathrm{N}(\mathrm{B}-T) \qquad (3.20)$$

where (x0, y0, z0) is the position of a magnetic source whose total magnetic field T is measured at (x, y, z) . The total field has a regional value B, and N is the degree of homogeneity (structural index), which is equivalent to n in Equation (3.13). The unknown coordinates (x_0, y_0, z_0) are estimated by solving a determined system of linear equations using a prescribed value for N with the least squares method. And a solution with a minimum standard deviation is found through using different tentative values for N.

In this study, the Euler deconvolution was used to determine the thickness of sediment for hydrocarbon potential of the study area.

3.4.4 Magnetic survey

Magnetic method is a geophysical technique that measures variations in the earth's magnetic field to determine the location of subsurface features. These non-destructive techniques have numerous applications in buried ferromagnetic objects (storage drums, pipes). Magnetic field variation can be interpreted to determine an anomaly's depth, geometry and magnetic susceptibility (Mickus, 2002).

Most common rock-forming minerals exhibit a very low magnetic susceptibility and rocks owe their magnetic character to the generally small proportion of magnetic minerals that they contain, Kearey and Brooks (1991). There are only two geochemical groups which provide such minerals. The iron-titanium-oxygen group possesses a solid solution series of magnetic minerals from magnetite (Fe_3O_2) to ulvospinel (Fe_2TiO_4) (Kearey, 2002). The other common iron oxide, haematite *(Fe_2O_3)* is anti-ferromagnetic and thus does not give rise to magnetic anomalies unless a parasitic anti-ferromagnetism developed. The iron sulphur group provides the magnetic mineral pyrrhotite *($FeS+x$, $0 > x < 0.15$)* whose magnetic susceptibility is dependent upon the actual composition. By far the most common magnetic mineral is magnetite, which has a curie temperature of 578^{o}C. The magnetic behavior of most rocks therefore, is dependent on their magnetite content (Moskowitz *et al*., 1998).

Basic igneous rocks are usually highly magnetic due to their relatively high magnetite content. The proportion of the magnetite in the igneous rocks tends to decrease with increasing acidity so that acidic igneous rocks, although variable in their magnetic behaviour, are usually less magnetic than basic rocks. Metamorphic rocks are also variable in their magnetic character. If the partial pressure of oxygen is relatively low, magnetite becomes reabsorbed and the iron and oxygen are incorporated into other mineral phases as the grade of metamorphism increases. Relatively high oxygen partial pressure can, however, result in the formation of magnetite as an accessory mineral in metamorphic reactions.

Generally, the magnetite content and, hence, the susceptibility of rocks are extremely variable and there can be considerable overlap between different lithologies,(Kearey and Brookes 1991).

Common causes of magnetic anomalies include dykes, faulted, folded or truncated sills and lava flows, massive basic intrusions, metamorphic basement rocks and magnetite ore bodies, Kearey and Brookes, (1991). Magnetic anomalies range in amplitude from a few tens of nano-teslas (nT) over deep metamorphic basement to several thousand nT over basic intrusions and may reach an amplitude of several thousand nT over magnetite ores, (Kearey and Brookes,1991).

Magnetic measurements for exploration are acquired from the ground, in the air, on the ocean, in space, and down boreholes, covering a large range of scales and for a wide variety of purposes. Measurements acquired from all but the borehole platform focus on variations in the magnetic field that are produced by lateral variations in the magnetization of the crust. Borehole measurements focus on vertical variations within the vicinity of the borehole.

3.4.5 Aeromagnetic survey

An aeromagnetic survey is a common type of geophysical survey carried out using a magnetometer aboard or towed behind an aircraft. This principle is similar to magnetic survey carried out with a hand-held magnetometer but allows much larger area of the earth’s surface to be covered quickly for regional reconnaissance. The aircraft typically flies in a grid-like pattern with height and line spacing determining the resolution of the data (and cost of the survey per unit area) (Edeh *et al*., 2017).

Majority of the magnetic surveys are carried out in the air, with the sensor towed in a housing known as a ‘bird’ to move the instrument from the magnetic effect of the aircraft or fixed in a ‘stinger’ in the tail of the aircraft, in which case inboard coil installations compensate for the aircraft magnetic field.

Aeromagnetic surveying is rapid and cost effective, typically costing some 40% less per line kilometre than a ground survey, Kearey and Brookes (1991). Vast areas can be surveyed rapidly without the cost of sending a field party into the survey area and data can be obtained from areas inaccessible to ground survey.

The main advantages of aeromagnetic surveys result from the great speed of surveying, which is an advantage in itself. Erratic magnetic features near surface are reduced or even eliminated by height of the aircraft. Also, operational problems associated with irregular terrains are eliminated. Finally, aeromagnetic surveys can be done over water and regions which are inaccessible for ground work.

While aeromagnetic surveys are extensively used as reconnaissance tools, there has been an increasing recognition of their value in evaluating prospective areas by virtue of the unique information they provide (Kearey and Brooks, 1991). The roles of aeromagnetic surveys are as follows:

- delineation of volcano-sedimentary belts under sand of other recent cover, or in strongly metamorphosed terrains when recent lithologies are otherwise unrecognizable.
- recognition and interpretation of faulting, shearing and fracturing not only as potential hosts for a variety of minerals, but also an indirect guide to epigenetic, stress related mineralisation in the surrounding rocks.
- identification and delineation of post-tectonic intrusive. Typical of such targets are zoned synite or carbonite complexes, kinerlites, tin-bearing granites and mafic intrusions.
- direct detection of deposits of certain ores.

3.4.6 Ground survey

Ground and airborne magnetic surveys are used at just about every conceivable scale and for a very wide range of purposes. In exploration, they historically have been employed chiefly in the search for minerals. Regional and detailed magnetic surveys continue to be a primary mineral exploration tool in the search for a diversity of commodities, such as iron, base and precious metals, diamonds, molybdenum, and titanium. Ground surveys historically, and primarily airborne surveys today, are used for the direct detection of mineralization, such as FeO-Cu-Au deposits, skarns, massive sulfides, and heavy mineral sands, for locating favorable host rocks or environments, such as carbonatites, kimberlites, porphyritic intrusions, faulting, and hydrothermal alteration, and for general geologic mapping of prospective areas.

3.4.7 The geomagnetic field

Magnetic anomalies caused by rocks are localised effects superimposed on the normal magnetic field of the earth, (Kearey and Brookes, 1991). Consequently, the knowledge of the behaviour of the geomagnetic field is necessary in both reductions of magnetic data to a suitable datum and in interpretation of the resulting anomalies. The geomagnetic field is geometrically very complex and exhibits irregular variations in orientation, magnitude, latitude, longitude and time.

At any point on the earth's surface, a freely suspended magnetic needle will assume a position in space in the direction of ambient geomagnetic field. This will generally be an angle to both the vertical and geographic north. In order to describe the magnetic field vector, use is made of descriptors known as the magnetic field elements (Figure 1.1). The total field vector $\boldsymbol{F_e}$ has a vertical component $\boldsymbol{Z_e}$, and a horizontal component $\boldsymbol{H_e}$ in the direction of magnetic north. The dip of $\boldsymbol{F_e}$ is the inclination $\boldsymbol{I}$ of the field and the horizontal angle between geographic and magnetic north is the declination $\boldsymbol{D}$.

The geomagnetic field is often divided into three in relation to geophysics. These three parts are:

i. **The Main Field**: This is the major part of the geomagnetic field. It accounts for about 95% of the total geomagnetic field. Its variation with time is very slow. Several theories attribute its origin to electrical currents circulating in the outer core of the earth and it accounts for large scale regional variation in intensity and direction.

ii. **The External Field**: The external field is a small fraction of the main field, about 1-5% of the total geomagnetic field. It varies rapidly and sometimes randomly as compared with the main field. Its variations include sunspot circle (11 years), solar diurnal variation (about 24 hours with amplitude of about 30 gammas) and lunar diurnal variation (about 25 hours with amplitude of about 2 gammas) (Telford *et al.,* 1976).

It is also characterised by magnetic storm which is often transient and erratic with amplitude of up to 1000 gamma. It is thought to originate from the outside of the earth and it affects magnetic prospecting data (Telford *et al.,* 1976).

iii. **Variation of the Main Field**: This is often called the anomalous field. Variation in the main field is said to be caused by variations in the mineral content of the near surface rocks (Telford *et al.,* 1976). These anomalies are usually smaller than the main field but may occasionally be large enough to double the main field. The variations are relatively constant in space and time and are restricted to the upper part of the crust since the temperatures at depth beneath the crust should be very much higher than their curie temperatures (Telford *et al.,* 1976). They do not persist over great distances. The variation in the main field is often the target of magnetic exploration in applied geophysics.

iv. In magnetic prospecting, instruments exist that can measure any of the components $\boldsymbol{H_e}$ or $\boldsymbol{Z_e}$. Most aeromagnetic instruments measure the total field, $\boldsymbol{F_e}$. These include the Proton Procession Magnetometer and the Optical Pump Magnetometers. In this aeromagnetic study, only the total field is dealt with.

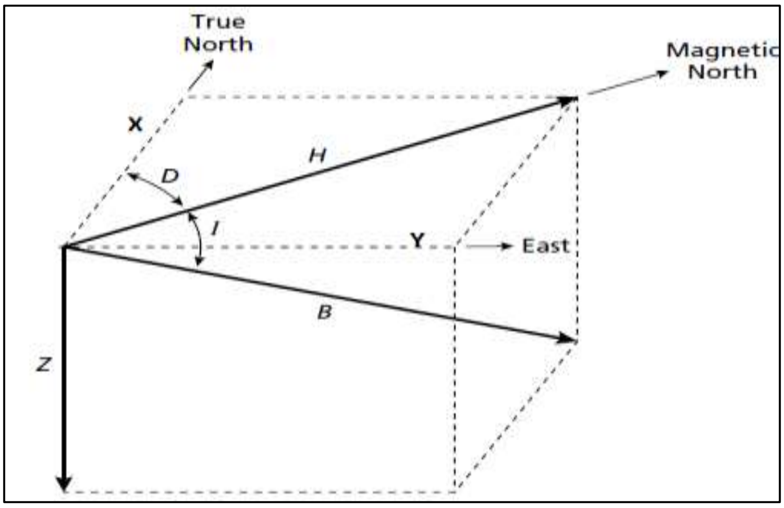

Figure 3.1: The geomagnetic elements (Kearey *et al.*, 2002).

3.4.8 Magnetic susceptibility

An un-magnetised steel needle assumes a particular configuration when freely suspended above the earth's surface due to the effect of induced magnetism of the earth. Once a material is placed within a magnetizing force field $\overrightarrow{H_f}$, the magnetic material will produce its own magnetization. This is induced magnetisation or polarization. The induced magnetic field of the material will appear to be created by a series of magnetic dipoles located within the magnetic material and oriented parallel to the direction of the induced field $\overrightarrow{H_f}$. The strength of the induced magnetic field of the material due to the inducing field is called the intensity of magnetisation $\vec{J}$.

Common magnets exhibit a pair of poles and are therefore referred to as dipoles. The *magnetic moment* M of a dipole with poles of strength m a distance l apart is given by

$$M = ml \qquad 3.21$$

The magnetic moment of a current-carrying coil is proportional to the number of turns in the coil, its cross-sectional area and the magnitude of the current, so that magnetic moment is expressed in Am^2. The intensity of induced magnetisation J_i of a material is defined as the dipole moment per unit volume of material:

$$J_i = \frac{M}{AL} \qquad 3.22$$

Where M is the magnetic moment of a sample of length L and cross-sectional area A. J_i is consequently expressed in Am^{-1}. In the c.g.s. system intensity of magnetisation is expressed in $emucm^{-3}$ (emu = electromagnetic unit), where 1 $emucm^{-3}$ = 1000 Am^{-1}. The induced intensity of magnetisation is proportional to the strength of the magnetising force H of the inducing field:

$$J_i = kH \qquad 3.23$$

Where k is the *magnetic susceptibility* of the material. Since J_i and H are both measured in ($Am^{-1)}$, susceptibility is dimensionless in the SI system. In the c.g.s. system susceptibility is similarly dimensionless, but a consequence of rationalising the SI system is that SI susceptibility values are a factor 4π greater than corresponding c.g.s. values (Kearey *et al.,* 2002).

3.4.9 Magnetic data enhancement

The beginning stages of magnetic data interpretation generally involve the application of mathematical filters to observed data. The specific goals of these filters vary, depending on the situation. The general purpose is to enhance anomalies of interest and/or to gain some preliminary information on source location or magnetization. Most of these methods have a long history, preceding the computer age. Modern computing power has increased their efficiency and applicability tremendously, especially in the face of the ever-increasing size of digital data associated with modern airborne surveys.

Most filter and interpretation techniques are applicable to both gravity and magnetic data. As such, when applicable, it is common to reference a paper describing a technique for filtering magnetic data when processing gravity data and vice-versa.

CHAPTER FOUR

4.0 RESULTS AND DISCUSSION

4.1 The Total Magnetic Intensity Map (TMI)

The total magnetic intensity map of the study area (part of Adamawa trough) after IGRF removal of 33,000 nT for the purpose of handling was produced in colour aggregates (Figure 4.1); with pink to red colour portraying positive (high) anomalies while green to blue depicts negative (low) anomalies. The Total Magnetic Intensity map of the study area exhibits both positive and negative anomalies ranging from -80.7 nT to 139.6 nT. The extreme northern part of the area is predominantly positive (high) anomaly and it also appear in some part of the study area. The presence of the high magnetic anomaly at the North eastern part of the study area might be as a result of basement intrusion into the sediment since the study area is majorly sedimentary basin. While the South eastern portion of the study area is dominated by negative (low) magnetic anomalies. The central part of the study area is dominated by mixtures of both high and low short wavelength closures which are high in frequency of occurrence.

4.2 Residual Map of the Study Area

Figure 4.2 is the residual map of the study area produced after the residual/regional separation. The regional was removed from the total magnetic intensity map (Figure 4.1) using polynomial fitting order of Oasis Montaj and the result produced the residual map. The residual map emphasis the short wavelength anomalies after the separation and show variations in magnetic signature ranging from magnetic value of -87.4 nT and 78.9 nT. Major structures delineated on this map trend NW-SE, NE-SW and E-W which agrees with the structures identified on Figure 4.2 The residual map was further subjected to quantitative analysis to estimate the depth to magnetic source for hydrocarbon maturation and accumulation.

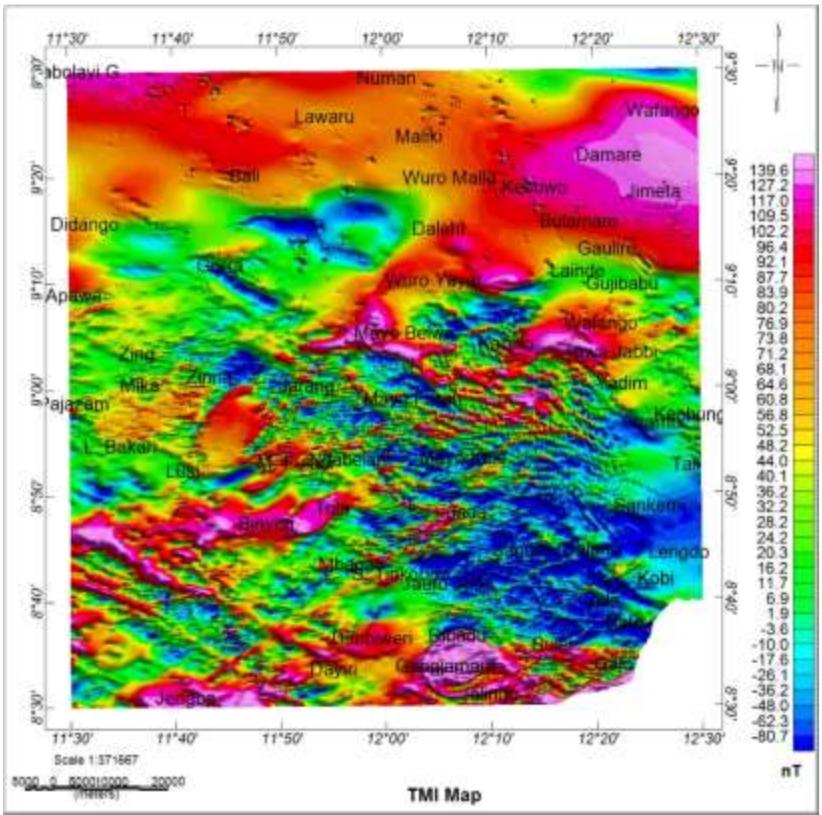

Figure 4.1: Total Magnetic Intensity (TMI) map

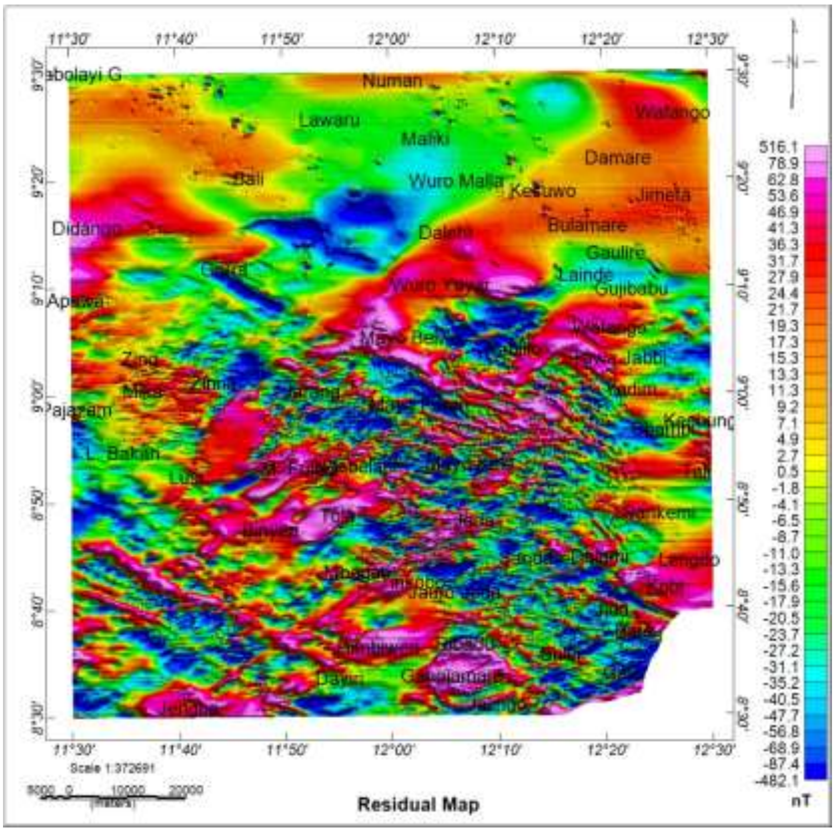

Figure 4.2: Residual map of the study area

4.3 Analytic Signal Map

Analytical Signal map reveals the variations in amplitudes of the magnetic anomalies which help in delineating the study area into regions of outcrop, intermediate structures and basement under the influence of thick sedimentation. Two major regions can easily be observed (Figure 4.3); regions whose amplitude responses are high which are predominantly basement intrusions with varying degree of deformations at the south eastern to the central part the study area; and regions whose amplitude are low, which depicts regions with relatively good sedimentation at the northern part of the study area.

4.4. Result of TMI Upward continued at 5 km and 10 km

Figure 4.4 and 4.5 is the total magnetic intensity map of the study area upward continued to the height of 5 km and 10 km respectively. At the height of 5 km and 10 km, the TMI map has been refined with little or no shorter wavelength anomalies noticeable. Close to four segments can be observed on this map. At the northern part and the extreme southern part of the map, the red to pink colour is more pronounced depicting crystalline rocks while the blue colour depicting thick sediment occupy the south-eastern part of the map and the greenish colour can be seeing at the central part of the study area . The yellow-pink colour dominates the northern and the western part of the map. This means that the effect of near surface magnetic anomalies has been subdued to some extent thereby exposing deep seated structures.

4.4.1 TMI upward continued at the height of 15 km and 20 km

The TMI map upward continued at the height of 15 km and 20 km are shown in the Figure 4.6 and Figure 4.7 respectively. The two maps exposed the total disappearance of the short wavelength anomalies (high frequency) thus enhancing longer wavelength, enhancing deep seated anomalies. The sedimentary portion of the study area occupy the south-eastern to eastern part of the study area. The maps also display that basement features are more at the western part of the study area.

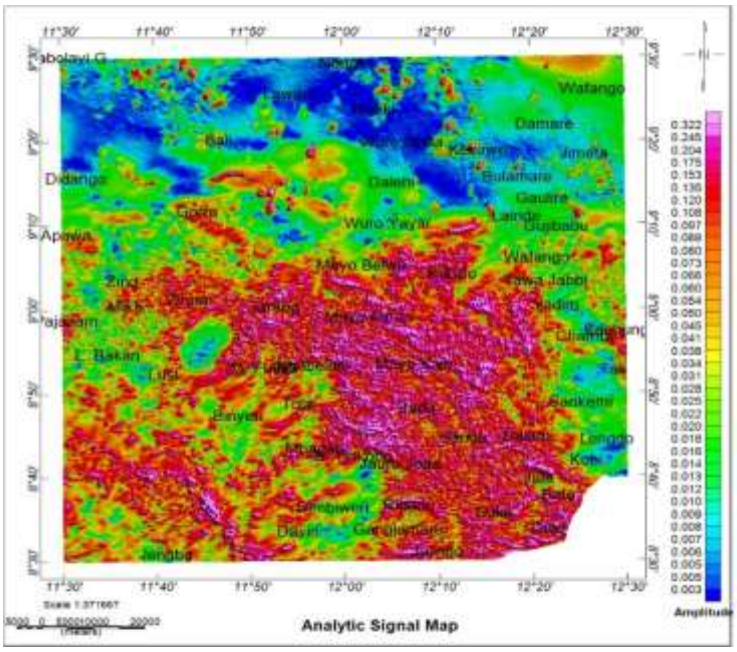

Figure 4.3: Analytic Signal Map of the Study Area

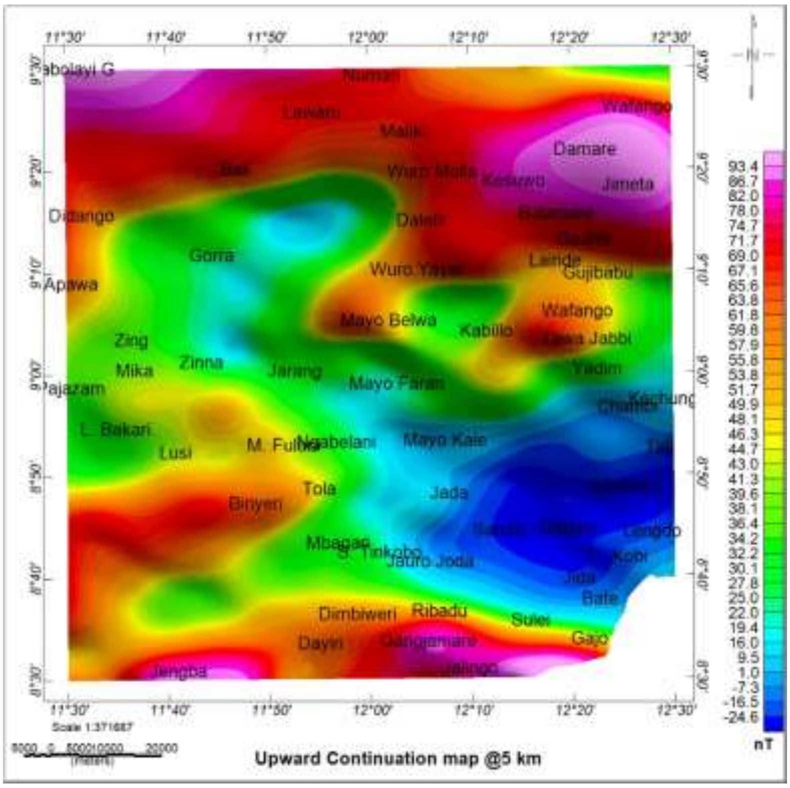

Figure 4.4: Upward Continuation map at the height of 5 km

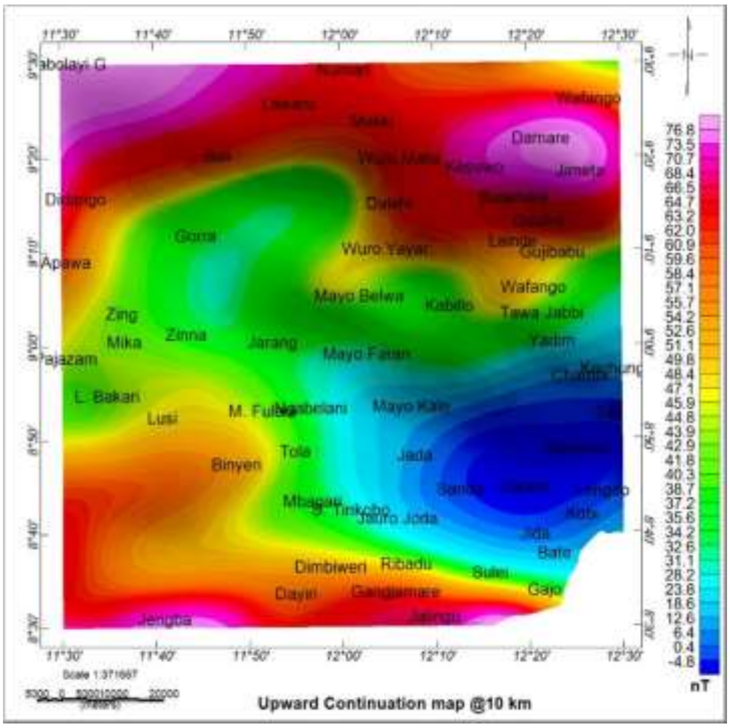

Figure 4.5: Upward Continuation map at the height of 10 km

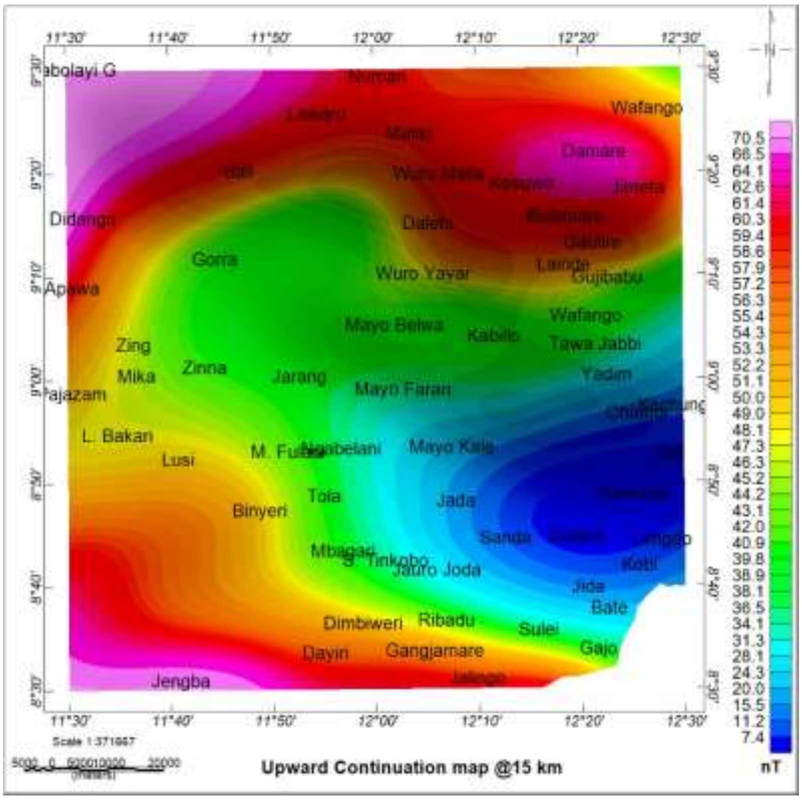

Figure 4.6: Upward continuation map at the height of 15 km

4.5 Results of Source Parameter Imaging (SPI)

The depth to top of magnetic basement of the study area was estimated using source parameter imaging (SPI). SPI gives a conspicuous image of the anomalies with respect to their depth. Figure 4.7 is the Source parameter imaging map and was produced in aggregates of colours; red to pink depicting shallow depth; green colour depicting intermediary depth and blue colour depicting thick sediments. Shallow and deeper depths were obtained from the results of the SPI; the shallow depths ranging from 64.9 m to 174.6 m at the southern to the central part of the study area which corresponds to Jada while maximum depth ranges from 1075.0 m to 4420.7 m at the north-eastern part of the study area which corresponds to Numal. Since the maximum depth of 3 km and above in a rift basin is sufficient for hydrocarbon maturation and accumulation (Adewumi *et al.*, 2017). Hence, the maximum sedimentary thickness of 4420.7 m obtained from the study area (Adamawa trough) is sufficient for hydrocarbon maturation and accumulation and a good pointer for petroleum exploration. Figure 4.3 corresponds with the SPI map with region of high amplitude corresponds with the regions of shallow depth probably of crystalline rock as a result of basement intrusion into the sediments and the regions of low amplitude corresponds to the regions of thick sediments.

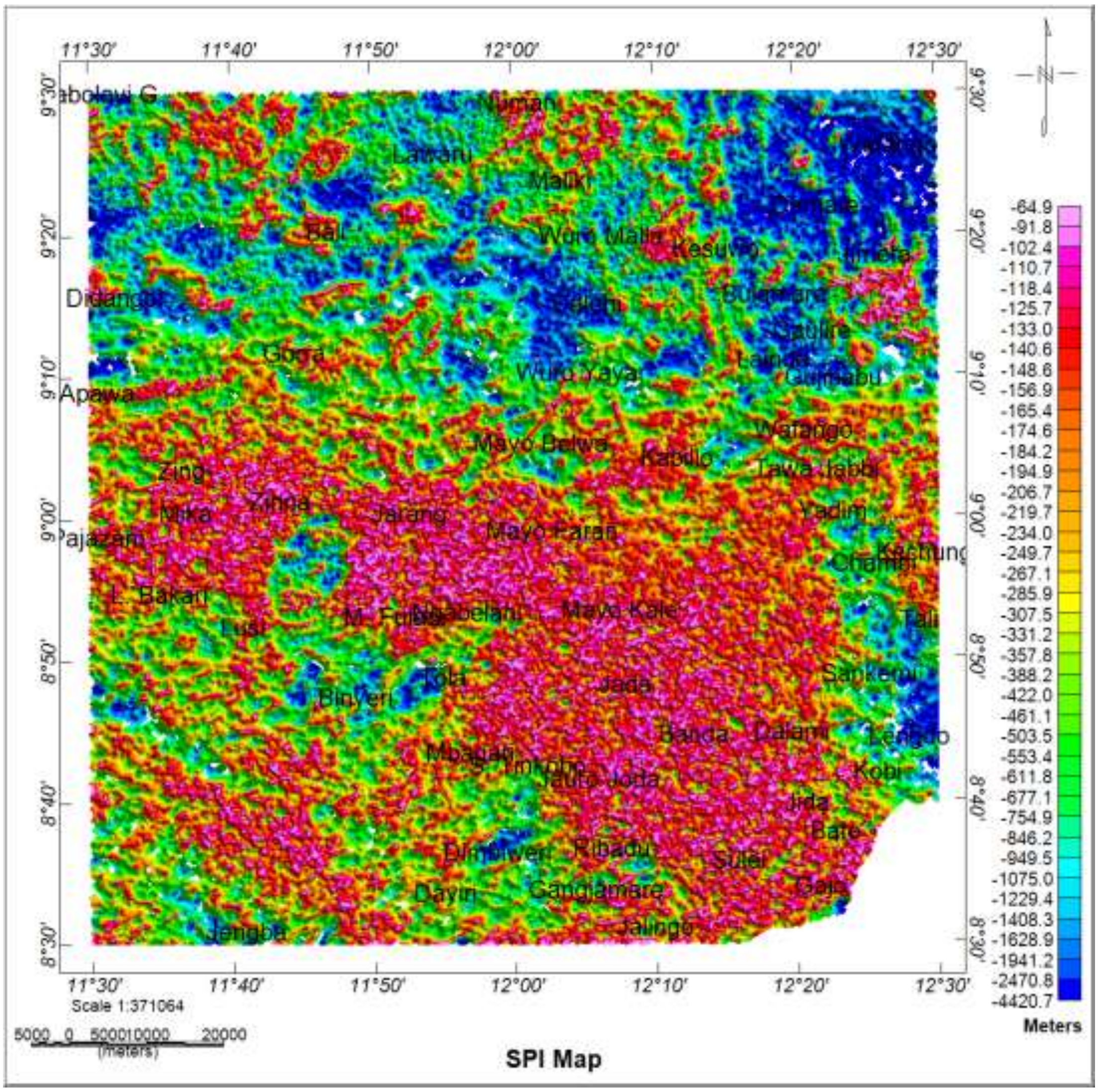

Figure 4.7: Source parameter imaging (SPI) map of the study area

4.6 Results of 3D Euler Deconvolution

The 3D Euler deconvolution method is one of the depths estimating automatic technique in determining the thickness of sediments and location of magnetic sources from observed magnetic field data. The Figure 4.8 represent the Euler deconvolution map produced from the study area. The pre-processed grids of the residual map (dx, dy and dz) were used to calculate the Euler depth with structural index 1. The Euler Depth map shows that the depth to magnetic sources (anomalies) ranges from 104.2 m to 4208.3 m. The Euler depth map agrees with the SPI map (Figure 4.16) and the Analytic signal map (Figure 4.3). The regions of shallow depth on the Euler depth map corresponds to the regions of shallow depth on Figure 4.17 and agrees with the regions of high amplitude on Figure 4.3 as result of basement intrusion into the sediments. While the region of deeper depth (thick sediments) on the Euler depth map corresponds to the regions of thick sediments on the Figure 4.16 and agrees with regions of low amplitude on Figure 4.3. The maximum depth of 4208.3 m obtained at the North eastern part of the study area from the Euler solutions is sufficient for hydrocarbon maturation and accumulation and a good indicator for petroleum exploration in the Adamawa trough.

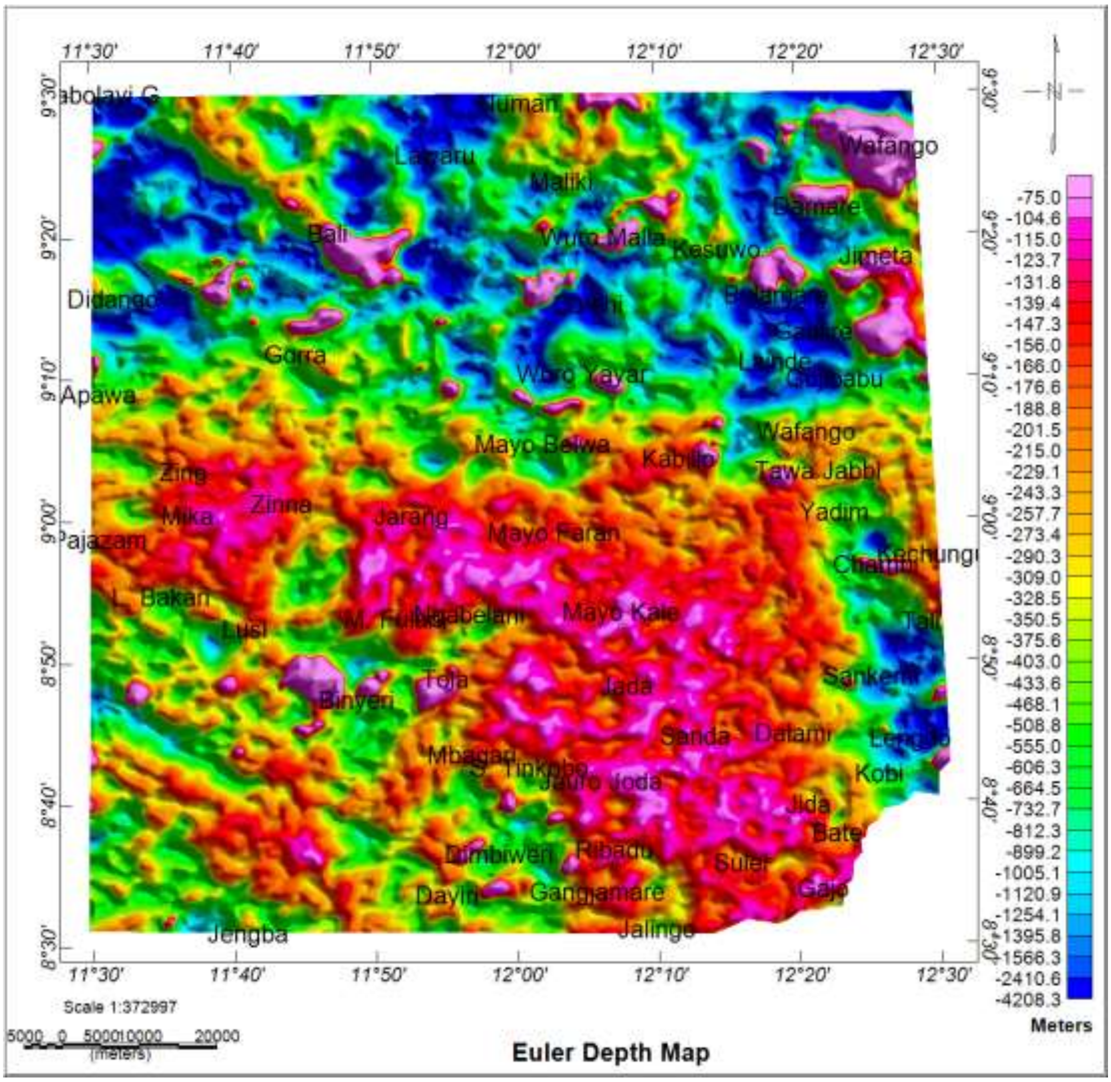

Figure 4.8: Euler depth map of the study area

4.7 Results from Spectral Analysis

This method was used in this present study to delineate the depth of the magnetic basement based on a moving data window by selecting the sharpest and therefore deepest straight-line segment of the power spectrum. A depth solution was calculated for the power spectrum derived from each grid sub-set located at the centre of the window. Overlapping the windows creates a regular, comprehensive set of depth estimates. The residual map (Figure 4.2) of the study area was divided into twelve (12) overlapping spectral blocks (A-L) of 55 x 55 km^2. Spectral analysis was performed on each block and a plot of spectrum energy against wavenumber was carried out using a program designed with Matlab software (Figure 4.9). The gradient from the plots give two depths; deeper and shallow depth and the results depth estimated are displayed on Table 4.1. The deeper depth obtained ranges from 1.69 km to 4.17 km with the maximum depth of 4.17 km found at the north-eastern part of the study area (Figure 4.9a). While the shallow depth ranges 0.82 km to 1.20 km and the shallowest depth could be found at the south-western part of the study area (Figure 4.9b). The region of high sedimentary thickness of above 4 km delineated agrees with the region of high sedimentary thickness delineated on Figure 4.7 and Figure 4.8. This thickness is enough for hydrocarbon maturation and accumulation for petroleum exploration.

Table 4.1: Spectral table of Deeper (Z_1) and Shallow (Z_2) Depth of the Study area

Blocks	Long. (Deg)	Lat (Deg)	Z_1(km)	Z_2 (km)
A	11.75	9.25	2.57	1.01
B	11.92	9.25	2.70	1.02
C	12.08	9.25	4.17	1.04
D	12.25	9.25	3.62	1.20
E	11.75	9.08	1.69	0.89
F	11.92	9.08	3.25	0.93
G	12.08	9.08	2.23	0.96
H	12.25	9.08	2.58	1.02
I	11.75	8.75	2.12	0.83
J	11.92	8.75	2.14	0.82
K	12.08	8.75	1.69	0.86
L	12.25	8.75	2.39	0.92

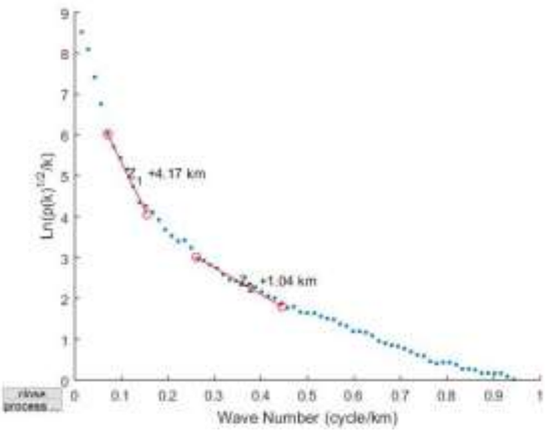

Figure 4.9a: Spectral plots for block C

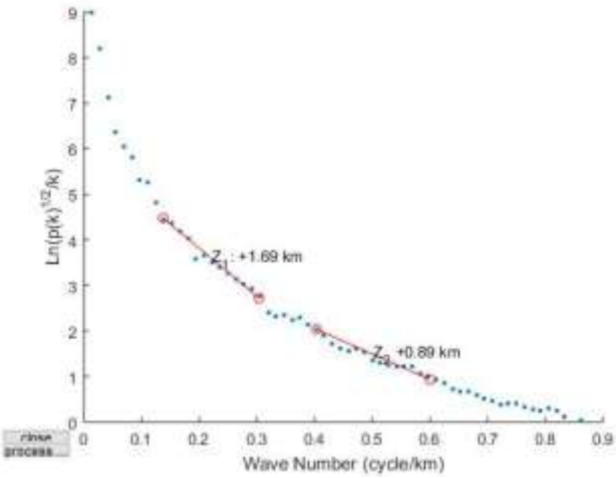

Figure 4.9b: Spectral plots for block E

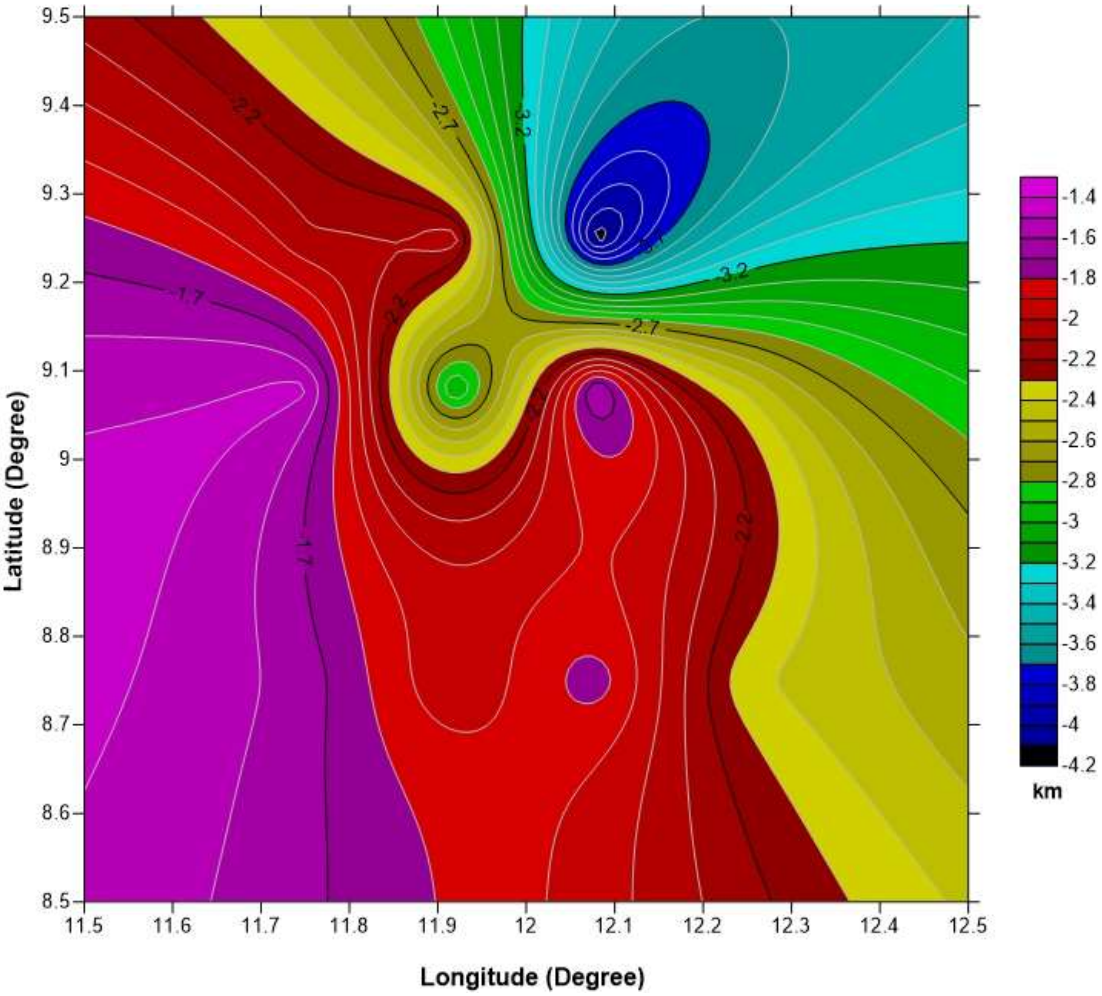

Figure 4.10: Contour map of the deeper depth of the Study area

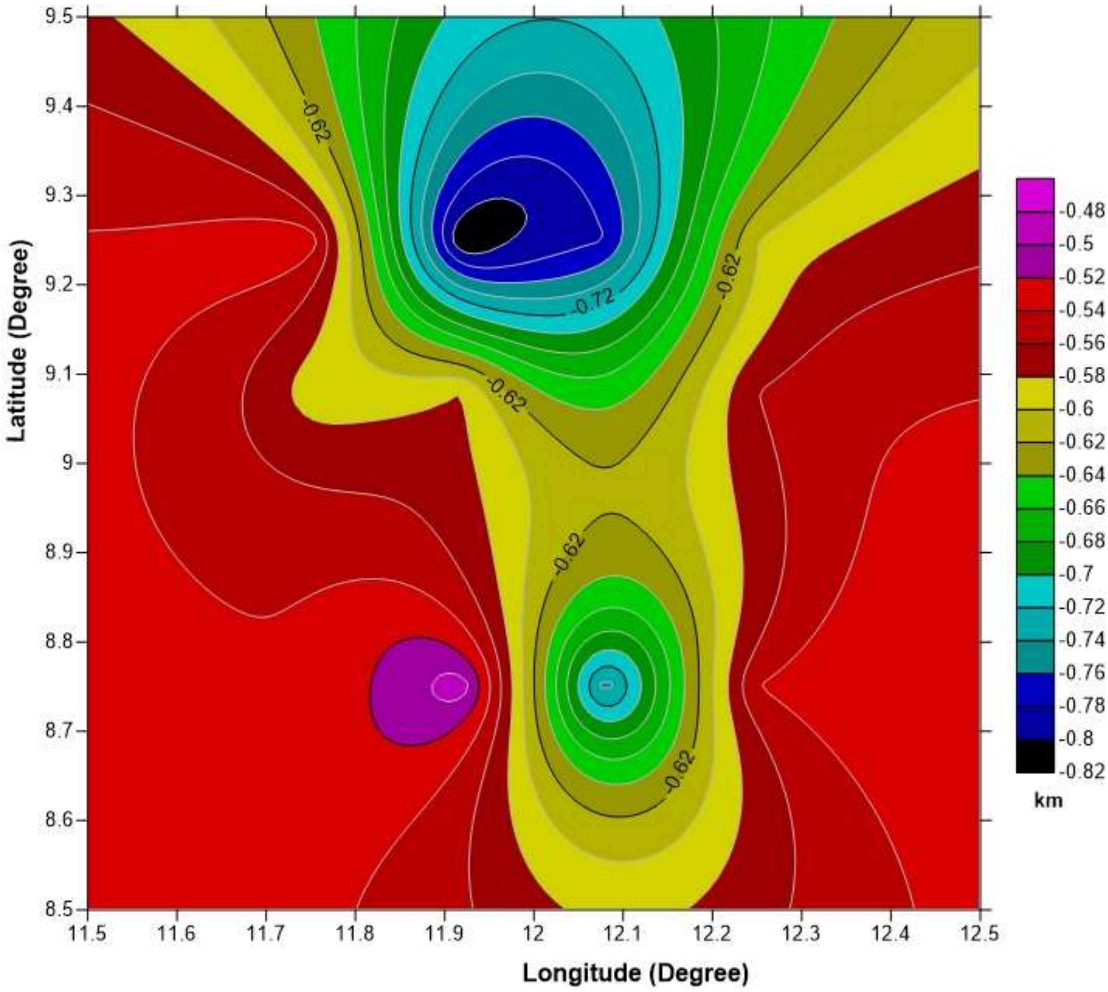

Figure 4.11: Contour map of the shallow depth of the study area

CHAPTER FIVE

5.0 CONCLUSION AND RECOMMENDATION

5.1 Conclusion

The aeromagnetic data of Adamawa trough has been analysed qualitatively using analytic signal and upward continuation techniques to delineate deeper subsurface structures and quantitatively using three depth estimating techniques; Source parameter imaging, Euler deconvolution and spectral method to estimate the thickness of sediments for hydrocarbon maturation and accumulation for petroleum exploration in the area.

The Total Magnetic Intensity map of the study area exhibits both positive and negative anomalies ranging from -80.7 nT to 139.6 nT. The extreme northern part of the area is predominantly positive (high) anomaly and it also appear in some part of the study area. The presence of the high magnetic anomaly at the north-eastern part of the study area might be as a result of basement intrusion into the sediment since the study area is majorly sedimentary basin. While the south-eastern portion of the study area is dominated by negative (low) magnetic anomalies. The central part of the study area is dominated by mixtures of both high and low short wavelength closures which are high in frequency of occurrence. Major structures delineated trends NE-SW, NW-SE and E-W.

The residual map emphasis the short wavelength anomalies after the separation and show variations in magnetic signature ranging from magnetic value of -87.4 nT and 78.9 nT. Major structures delineated on this map trend NW-SE, NE-SW and E-W which agrees with the structures identified on Figure 4.1. The residual map was further subjected to quantitative analysis to estimate the depth to magnetic source for hydrocarbon maturation and accumulation.

The analytic signal map reveal two major regions ; regions whose amplitude responses are high which are predominantly basement intrusions with varying degree of deformations at the southeastern to the central part the study area; and regions whose amplitude are low, which depicts regions with relatively good sedimentation at the northern part of the study area.

The TMI map was upward continued at different heights (5 km, 10 km, 15 km, 20 km, 25 km, 30 km, 35 km, 40 km, 45 km, 50 km, 60 km and 70 km) to delineate deep seated anomalies. At the height of 45 km, 50 km, 60 km and 70 km above flight level all the structures at this level are basement structures. The observed structures trend NW –SE and the lines delineated indicate lineament such as faults. This maps obviously expose the regional effects as a result, there is no sedimentation.

Three depth estimating techniques (SPI, Euler and Spectral method) were adopted to determine the depth to top of magnetic basement for hydrocarbon maturation and accumulation. Shallow and deeper depths were obtained from the results of the SPI; the shallow depths ranging from 64.9 m to 174.6 m at the southern to the central part of the study area which corresponds to Jada while maximum depth ranges from 1075.0 m to 4420.7 m at the north-eastern part of the study area which corresponds to Numal

The Euler Depth map shows that the depth to magnetic sources (anomalies) ranges from 104.2 m to 4208.3 m. The regions of shallow depth on the Euler depth map corresponds to the regions of shallow depth on Figure 4.17 and agrees with the regions of high amplitude on Figure 4.3 as result of basement intrusion into the sediments. While the region of deeper depth (thick sediments) on the Euler depth map corresponds to the regions of thick sediments on the Figure 4.16 and agrees with regions of low amplitude on Figure 4.3. The maximum depth of 4208.3 m obtained at the north-eastern part of the study area from the Euler solutions is sufficient for hydrocarbon maturation and accumulation and a good indicator for petroleum exploration in the Adamawa trough.

The spectral analysis generated two depths; the deeper depth which ranges from 1.48 km to 4.17 km with the maximum depth of 4.17 km found at the north-eastern part of the study area (Figure 4.19a) and the shallow depth ranges 0.42 km to 0.82 km and the shallowest depth could be found at the south-western part of the study area (Figure 4.19b). The region of high sedimentary thickness of above 4 km delineated agrees with the region of high sedimentary thickness delineated on Figure 4.16 and Figure 4.17.

5.2 Recommendation

The region with maximum sedimentary thickness of 4 km and above at the north-eastern part of the study area should be subjected to extensive geophysical method such as seismic reflection that gives a better image of the subsurface structures for petroleum exploration.

REFERENCES

Abdullahi, U.A., Ugwu, G.Z., & Ezema, P. O. (2014). Magnetic exploration of the upper and Lower Benue Trough for metallic deposits and hydrocarbons using 2D/3D. *Journal of Natural Sciences Research,* 4, 41-46

Adebanji K. Adegoke (2012) Biostratigraphy and depositional environment of the sediments in Borno Basin, North Eastern Nigeria. Indian Journal of Science and Technology 5(6) 2800-2809

Ajakaiye, D. E. (1981). Geophysical investigations in the Benue trough-a review. *Earth Evolution Sciences* 2,110-125.

Ajakaiye, D. E., Hall, D. H., Millar, T. W., Verheijen, P. J. T., Awad, M. B., & Ojo, S. B. (1986). Aeromagnetic anomalies and tectonic trends in and around the Benue Trough, Nigeria. *Nature*, *319*(6054), 582-584.

Ajayi, C. O., & Ajakaiye, D. E. (1981). The origin and peculiarities of the Nigerian Benue Trough: another look from recent gravity data obtained from the Middle Benue. *Tectonophysics*, *80*(1-4), 285-303.

Alagbe, O. A. & Sunmonu, L. A., (2014), Interpretation of aeromagnetic data from upper Benue basin, Nigeria using automated techniques *Journal of Applied Geology and Geophysics (IOSR-JAGG* . Volume 2, Issue 5, PP 22-40

Aldana, M., Costanzo-Alvarez, V., & Díaz, M. (2003). Magnetic and mineralogical studies to characterize oil reservoirs in Venezuela. *The Leading Edge*, *22*(6), 526-529.

Benkhelil, J. (1989). The origin and evolution of the Cretaceous Benue Trough (Nigeria). *Journal of African Earth Sciences (and the Middle East)*, *8*(2-4), 251-282.

Bhattacharrya, B.K. & Navolio. (1976). A fast fourier transform method for rapid computation of gravity and magnetic anomalies due to arbitrary bodies. Geophys. Prospecting, Vol. 24, pp. 633–649

Carter, J. D., Barber, W., Tait, E. A., & Jones, G. P. (1963). The Geology of parts of Adamawa, Bauchi and Bornu Provinces in north-eastern Nigeria. Bulletin Geological Survey Nigeria, 30, 1-99.

Chinwuko A. I., Onwuemesi A. G., Anakwuba E. K., Onuba L. O. & Nwokeabia N .C. (2012) Interpretation of Aeromagnetic Anomalies over parts of Upper Benue Trough and Southern Chad Basin, Nigeria *Advances in Applied Science Research,* 3 (3):1757-1766

Costanzo-Alvarez, V., Aldana, M., Aristeguieta, O., Marcano, M. C., & Aconcha, E. (2000). Study of magnetic contrasts in the Guafita oil field (South-Western

Venezuela). *Physics and Chemistry of the Earth, Part A: Solid Earth and Geodesy*, *25*(5), 437-445.

Cratchley, C. R., Louis, P., & Ajakaiye, D. E. (1984). Geophysical and geological evidence for the Benue-Chad Basin Cretaceous rift valley system and its tectonic implications. *Journal of African Earth Sciences (1983)*, *2*(2), 141-150.

Dobrin, M. B., & Savit, C. H. (1988). Introduction to Geophysical Prospecting McGraw-Hill Book Co. *New York (867 pp.)*.

Edeh, G. U., Abangwu, J. U., Okwesili, A. N., Ossai, M. N., & Obiora, D. N. (2017) Estimation of depth to magnetic source bodies of Nsukka and Udi areas using spectral analysis approach. *International Journal of Physical Sciences*, *12*(13), 146-162.

Fitton, J. G. (1980). The Benue trough and Cameroon line—a migrating rift system in West Africa. *Earth and Planetary Science Letters*, *51*(1), 132-138.

Fuller, B. D. (1967) Two-Dimensional Frequency Analysis and Design of

Geophysics 35, pp 293-30 *Geophysics*, 30 (3): 891-902Grid Operators. *Mining Geophysics (SEG, Tulsa),* Vol 11. 658-708

Gunn, P. J., & Dentith, M. C. (1997). Magnetic responses associated with mineral deposits. *AGSO Journal of Australian Geology and Geophysics*, *17*, 145-158.

Haruna, I. V., Ahmed, H. A., & Ahmed, A. S. (2012). Geology and tectono-sedimentary disposition of the Bima sandstone of the Upper Benue Trough (Nigeria): Implications for sandstone-hosted Uranium deposits. *Journal of Geology and Mining Research*, *4*(7), 168-173.

Hood, P. 1965: Gradient Measurements in Aeromagnetic Surveying:

Kearey, P., Brooks, M. & Hill, I. (2002) *An Introduction to Geophysical Exploration*. Blackwell Science Ltd., Oxford.

Kearey, P., Brooks, M., & Hill, I. (2002). *An Introduction to Geophysical Exploration*. London: Blackwell Science Ltd.

Kearey, P., Brooks, M., & Hill, I. (2002). *An introduction to geophysical exploration* (Vol. 4). John Wiley & Sons.

Keary, P. & Brooks, M. (1991) *An Introduction to Geophysical Exploration*. 2nd Edition, Blackwell Scientific Publications, Oxford, 254 p.179.

Keary, P., & Brooks, M. (1991). An Introduction of Geophysical Prospecting.

Le Roux J. P (1993). Genesis of stratiform U-Mo deposits in the Karoo Basin of South Africa. Ore Geol. Rev. 7:485-509

Le Roux J.P (1991). Flume experiments on permeability and organic matter as related to the genesis of uranium deposits in the Beaufort Group. S. Afr. J. Geol. 94:212-219.

Le Roux JP (1993). Genesis of stratiform U-Mo deposits in the Karoo Basin of South Africa. Ore Geol. Rev. 7:485-509.

Mickus, K. (2002). Magnetic Method. *Exploration Geophysics*.

Mickus, K., (2002) Magnetic method presented at the first international conference on the application of Geophysical methodologies and NDT to transportation facilities and infrastructures Pg 1-9,

Milligan, P & Gunn, P. (1997) Enhancement and presentation of airborne geophysical data. AGSO J. Australian Geol. & Geophy., 17(2): 63-75.

Mohammed, A. G., & Mustapha, A. (2014). Evaluation of the magnetic basement depth over parts of Bajoga and Environs, Northeastern Nigeria by Stanley's Method. *IOSR Journal of Applied Geology and Geophysics (IOSR-JAGG) e-ISSN*, 2321-0990.

Nabighian, M. N., (1972). The analytical signal of two-dimensional magnetic bodies with polygonal cross –section: Its properties and use for automated anomaly interpretation: *Geophysics*, 37, 507-517

Nwachukwu, S. O., (1972). The tectonic evolution of the Southern portion of the Benue Trough, Nigeria. Geological magazine (109) pp.411-419.

Nwogbo, P. O. (1997). Mapping the shallow magnetic sources in the Upper Benue basin of Nigeria from aeromagnetic spectra. *Africa Geoscience Review*, *4*, 325-334.

Nwosu O.B. (2014). Determination Of Magnetic Basement Depth Over Parts Of Middle Benue Trough By Source Parameter Imaging (SPI) Technique Using HRAM. *International Journal Of Scientific & Technology Research*, 3(1), 262-271.

Offodile, M. E. (1976). The geology of the middle Benue, Nigeria. *Palaeontological Institute, University Uppsala, Special Publication*, *4*, 1-166.

Ofoegbu C. O. (1988). An Aeromagnetic Study of part of the Upper Benue Trough, Nigeria. *Journal African Earth Sciences*,7(1), 77-90.

Ofoegbu, C. O. (1984). Interpretation of aeromagnetic anomalies over the Lower and Middle Benue Trough of Nigeria. *Geophysical Journal International*, *79*(3), 813-823.

Ogundipe, I. E., & Obasi, R. A. (2016). Geology and mineralisation in the Albian Sediments of the Benue Trough, Nigeria. *British Journal of Earth Sciences Research*, *4*(3), 1-15.

Oha, I. A., Okonkwo, I. A., & Dada, S. S. (2020). Wrench tectonism and intracontinental basin sedimentation: a case study of the moku sub-basin, upper Benue trough, Nigeria. *J. Geogr. Geol.*, *12*(1), 65-75.

Oha, I. A., Onuoha, K. M., Nwegbu, A. N., & Abba, A. U. (2016). Interpretation of high-resolution aeromagnetic data over southern Benue Trough, South Eastern Nigeria. *Journal of Earth System Science*, *125*(2), 369-385.

Okonkwo C. C., Onwuemesi A. G., Anakwuba E. K, Chinwuko A. I., Ikumbur B. E. and Usman A. O. (2012). Aeromagnetic Interpretation over Maiduguri and Environs of Southern Chad Basin, Nigeria *Journal of Earth Sciences and Geotechnical Engineering, vol.2, no. 3, 2012, 77-93*

Olade, M. A. (1975). Evolution of Nigeria's Benue Trough (Aulacogen): a tectonic model. *Geological magazine*, *112*(6), 575-583.

Onuoha, K. M., Ofoegbu, C. O., & Ahmed M.N. (1994).Spectral Analysis of Aeromagnetic Data Over the Middle Benue Trough, Nigeria. *Journal of Mining and Geology,* 30(2), 211-217.

Orajaka, S. O. (1972). Nigerian ore deposits [J]. *Mining. Mag*.

Osazuwa, I. B., Ajakaiye, D. E., & Verheiien, P. J. T. (1981). Analysis of the structure of part of the upper Benue rift valley on the basis of new geophysical data. *Earth Evolution Sciences* 2, 126-135.

Osazuwa, I. B., Ajakaiye, D. E., & Verheijen, P. J. T. (1969). Analysis of the structure of part of the Upper Benue Rift Valley on the basis of new geophysical data. *Tectonophysics*, *30,* 269-298.

Reid, A.B., Allsop, J.M., Granser, A., millett, A.J. & Somertom, I.W. (1990). Magnetic interpretation in three dimension using Euler deconvolution. Geophysics, Vol. 55, pp. 80–91.

Reynolds, J. M. (2011). *An introduction to applied and environmental geophysics*. John Wiley & Sons.

Roest, W. R., Verhoef, J. & Pilkington, M., (1992). Magnetic interpretation using 3-D analytical signal: *Geophysics,* 57,116-125.

Salako, K. A. (2014). Depth to basement determination using source parameter imaging (SPI) of aeromagnetic data: An application to upper Benue trough and Borno basin, Northeast, Nigeria. *Academic Research International*, 5(3): 74-86.

Salako, K. A., & Udensi, E. E (2013). Spectral depth analysis of parts of upper Benue trough and Borno basin, North-East Nigeria, using aeromagnetic data. *International Journal of Science and Research,* 2(8)48-55.

Spector A. & Grant F. S. (1970) Statisstical models for interpreting aeromagnetic data.

Steenland, N. C. (1965). Oil fields and aeromagnetic anomalies. *Geophysics*, *30*(5), 706-739.

Suh, C. E., Dada, S. S., & Matheis, G. (2000). Host rock geology and geochemistry of the Zona uranium occurrence, Peta Gulf Syncline (Upper Benue Trough), northeast Nigeria. *Journal of African Earth Sciences*, *31*(3-4), 619-632.

Telford, W. M., Telford, W. M., Geldart, L. P., Sheriff, R. E., & Sheriff, R. E. (1990). *Applied geophysics*. Cambridge university press.

Telford, W.M., Geldart, L.P. & Sheriff, R.E. (1990). *Applied Geophysics*, 2nd edition, Cambridge, London: Cambridge University Press

Thompson, D.T. (1982) Euler Depth- new technique for making computer assisted depth estimates of magnetic data. Geophysics, Vol. 47, pp. 31–37.

Thurston, J., Guillon, J.C. and Smith, R. (1999). Model-independent depth estimation with the SPI^{TM} method: 69th Annual International Meeting, SEG, Expanded Abstracts, pp. 403–406.

Thurston, J.B., & Smith, R.S. (1997). Automatic conversion of magnetic data to depth, dip and susceptibility contrast using the SPI^{TM} method. Geophysics. Vol. 62, pp. 807–813.

Thurston, J.B., Smith, R.S. & Guillon, J.C. (2002). A multimodel method for depth estimation from magnetic data: Geophysics, 67, pp. 555–561.

Yandoka, B. M. S., Abubakar, M. B., & Abdullah, W. H. Yola Sub-Basin, Northern Benue Trough, Ne Nigeria: A Mixed. *Journal of African Earth Sciences*, *96*, 168

APPENDIX

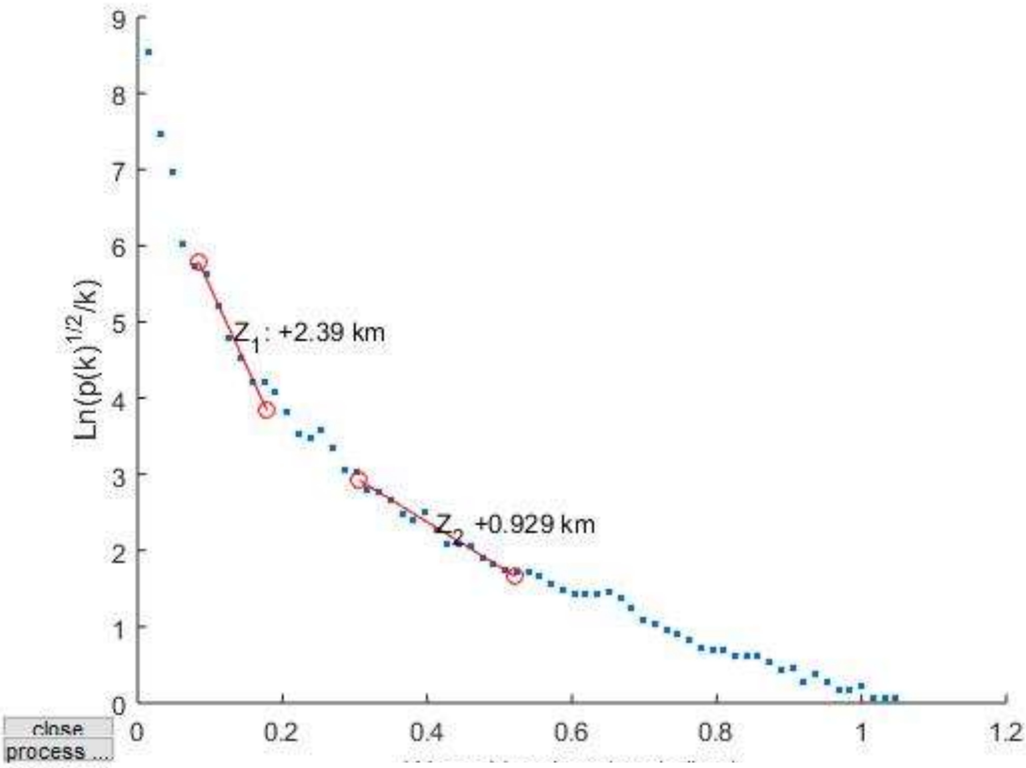

Z_1: +2.39 km
Z_2 +0.929 km
Ln(p(k)^{1/2}/k)
close
process ...

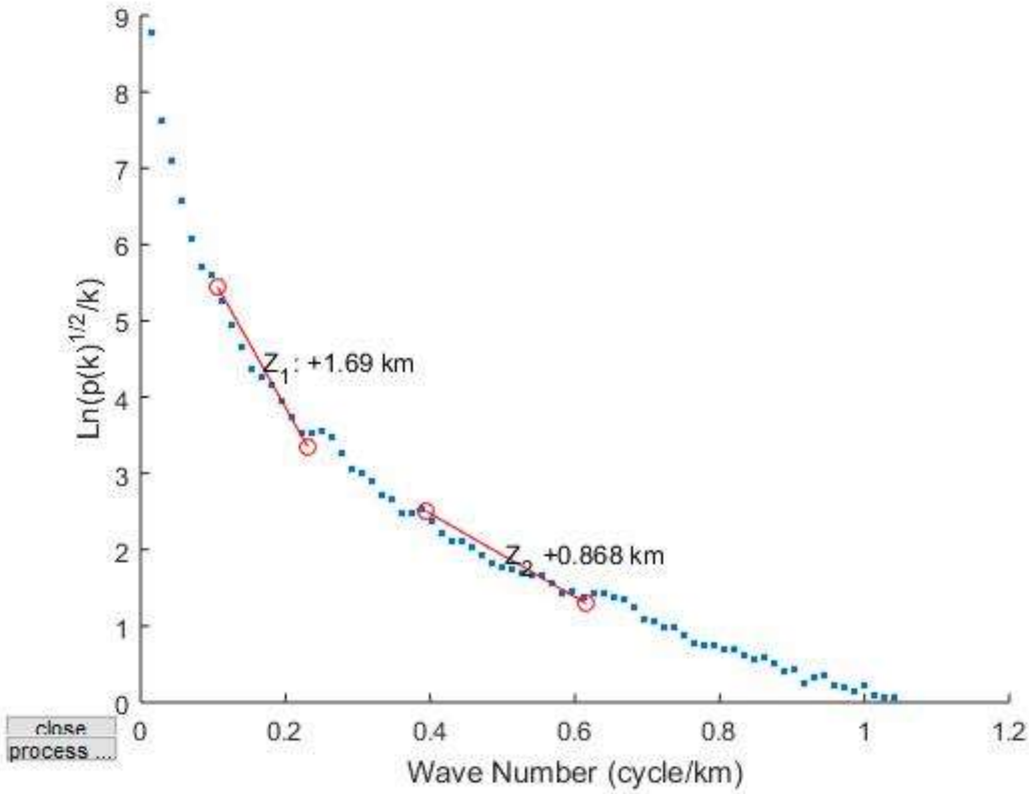

Z_1: +1.69 km
Z_2 +0.868 km
Ln(p(k)^{1/2}/k)
Wave Number (cycle/km)
close
process ...

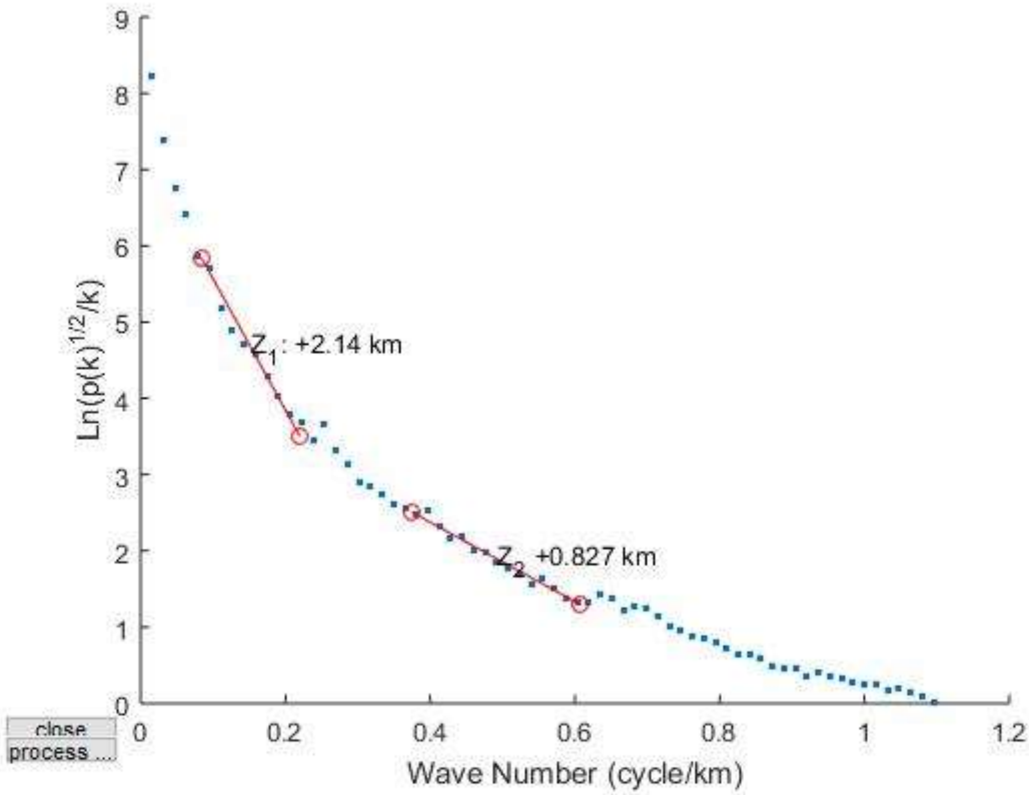

Ln(p(k)^1/2/k)
Z1: +2.14 km
Z2 +0.827 km
close
process ...
Wave Number (cycle/km)

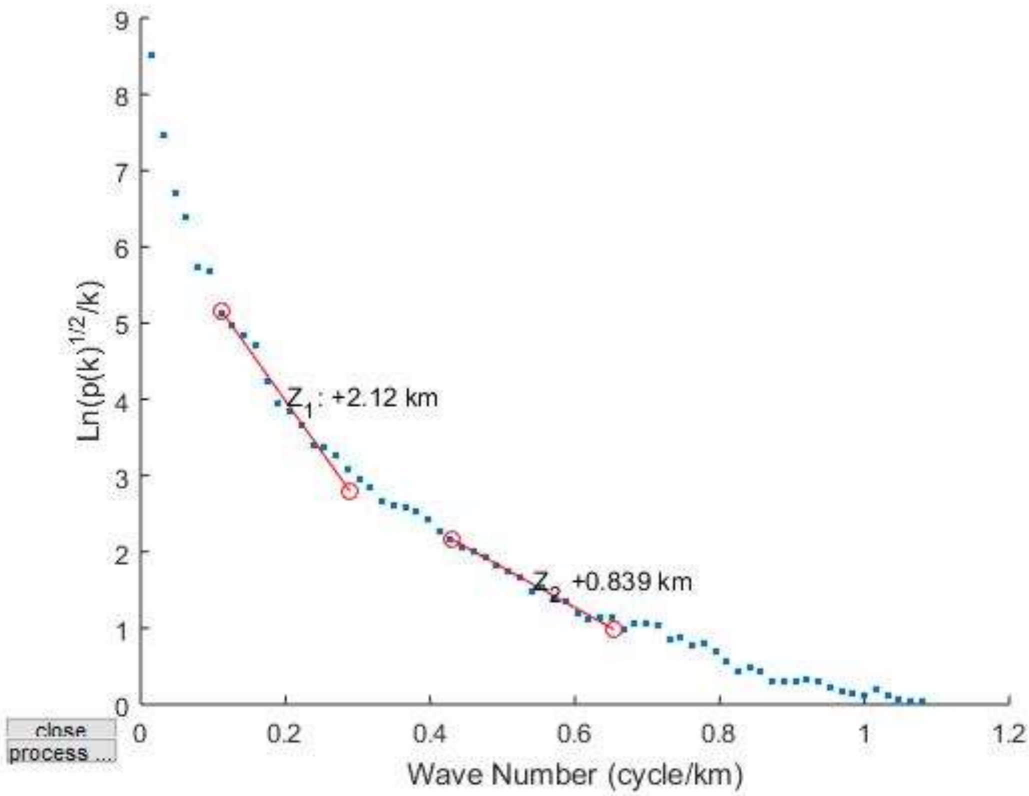

Ln(p(k)^1/2/k)
Z1: +2.12 km
Z2 +0.839 km
close
process ...
Wave Number (cycle/km)

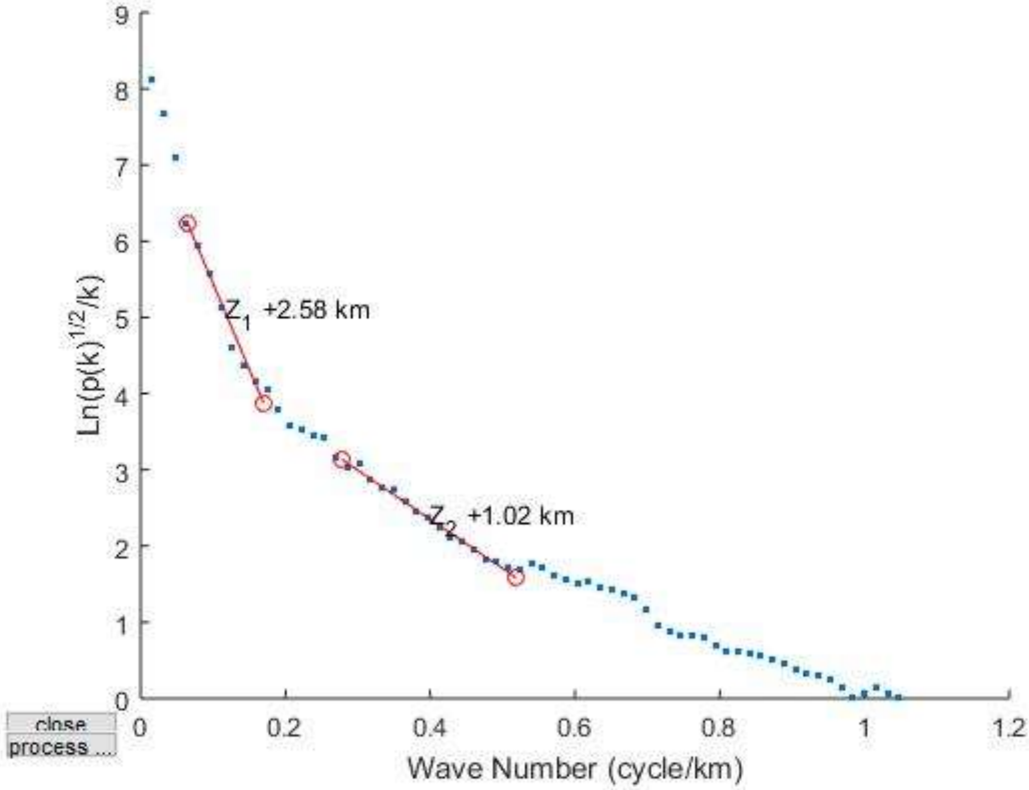

Ln(p(k)^1/2/k)
Wave Number (cycle/km)
Z1 +2.58 km
Z2 +1.02 km
close
process ...

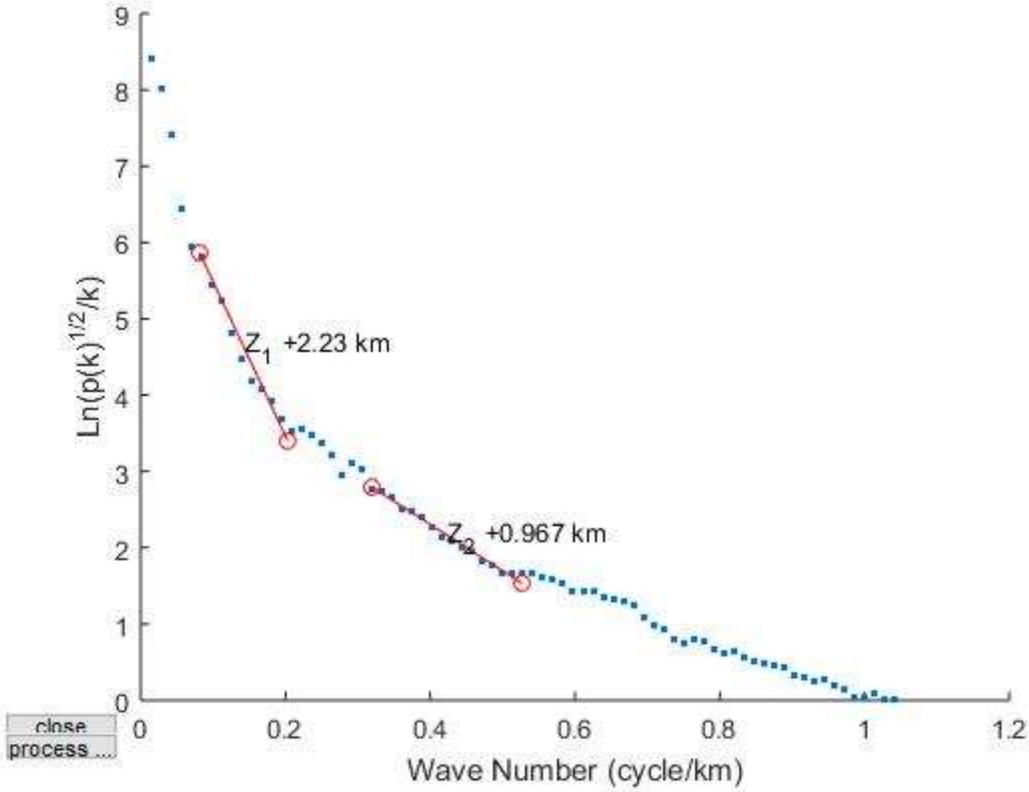

Ln(p(k)^1/2/k)
Wave Number (cycle/km)
Z1 +2.23 km
Z2 +0.967 km
close
process ...

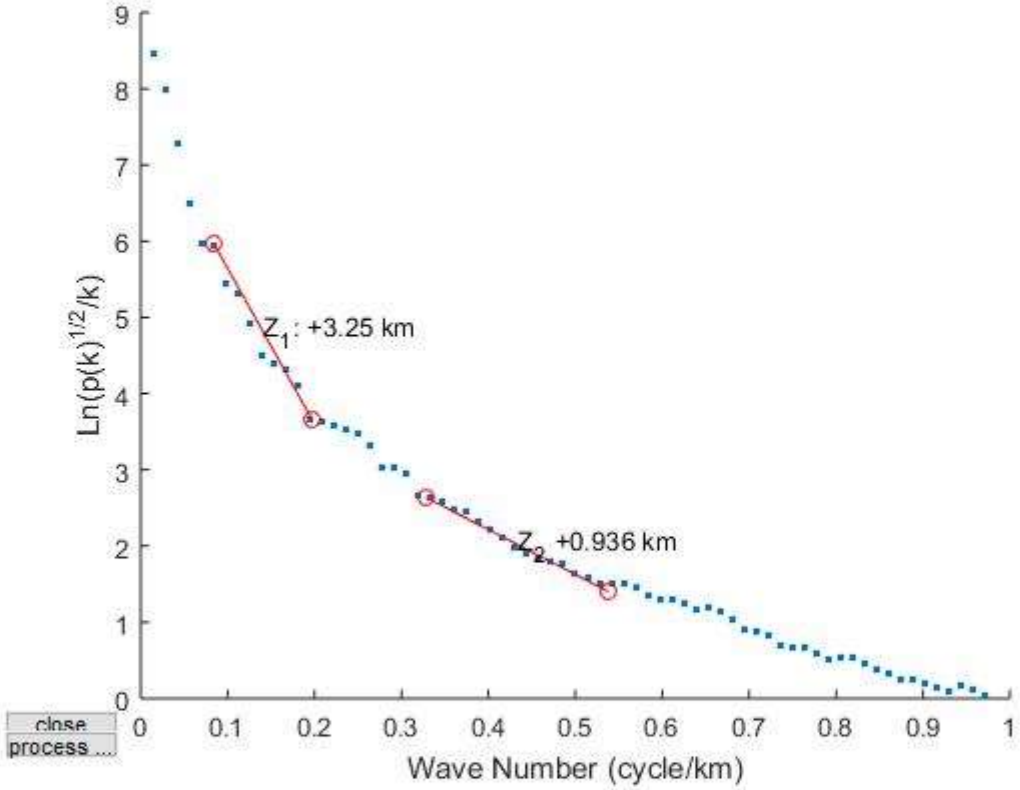
Ln(p(k)^1/2/k)
Z1: +3.25 km
Z2 +0.936 km
Wave Number (cycle/km)
close
process ...

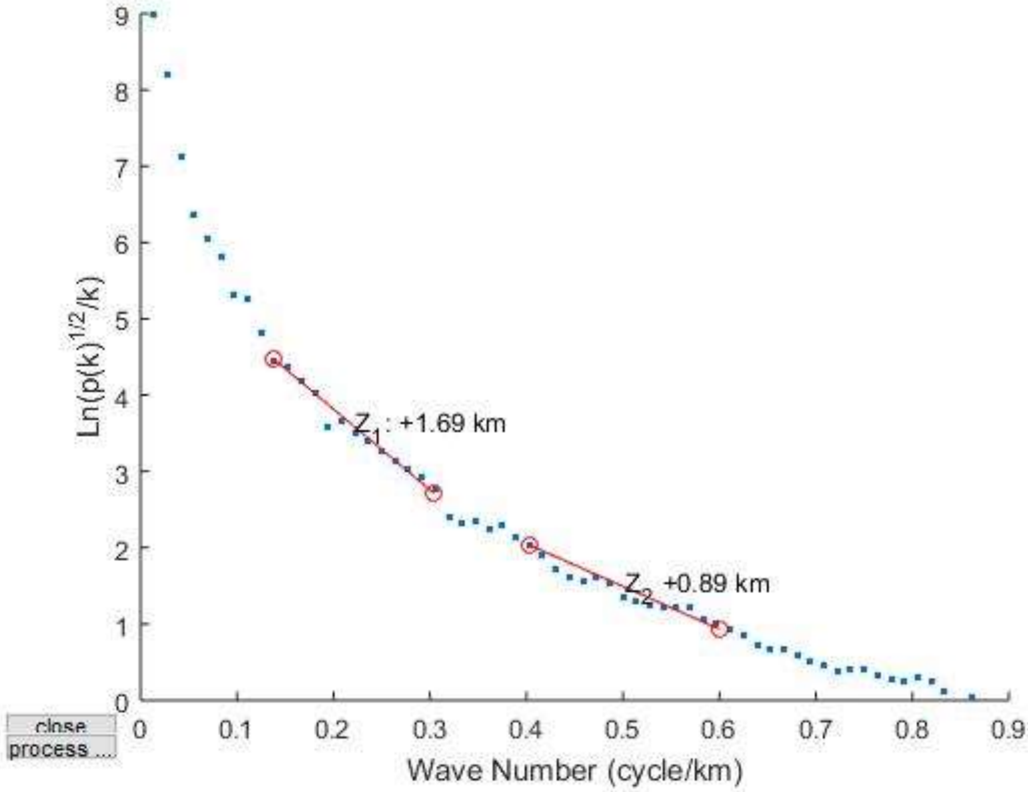
Ln(p(k)^1/2/k)
Z1: +1.69 km
Z2 +0.89 km
Wave Number (cycle/km)
close
process ...

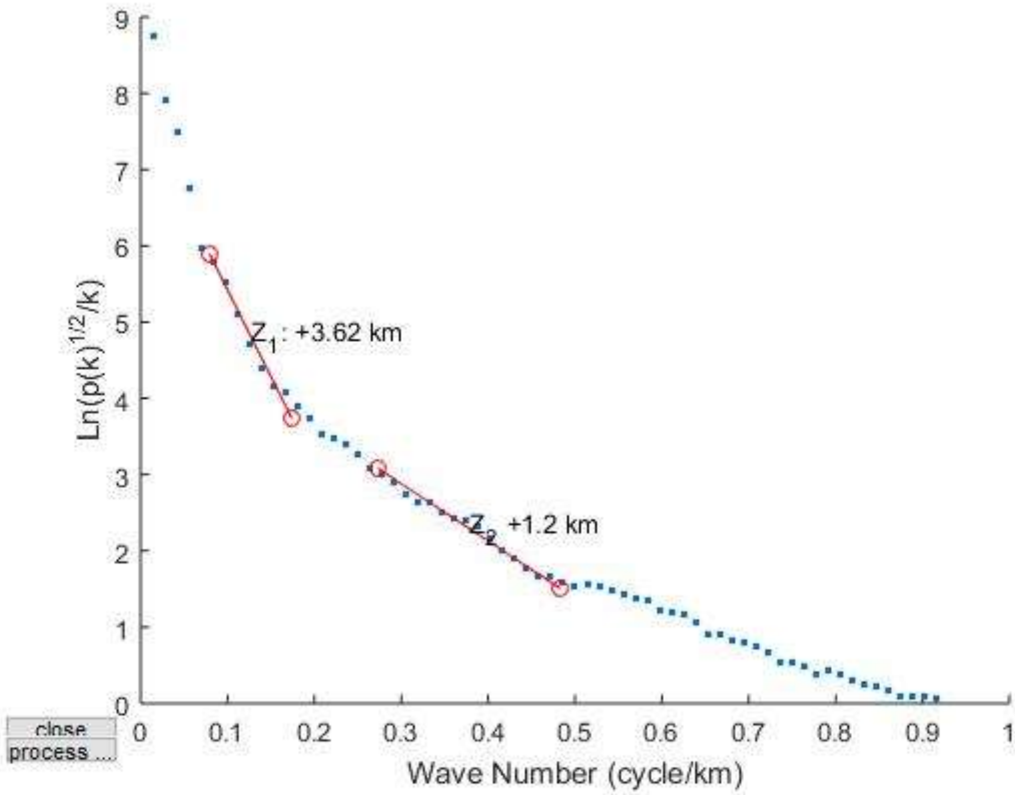

Ln(p(k)^1/2/k)
Z1: +3.62 km
Z2 +1.2 km
close
process ...
Wave Number (cycle/km)

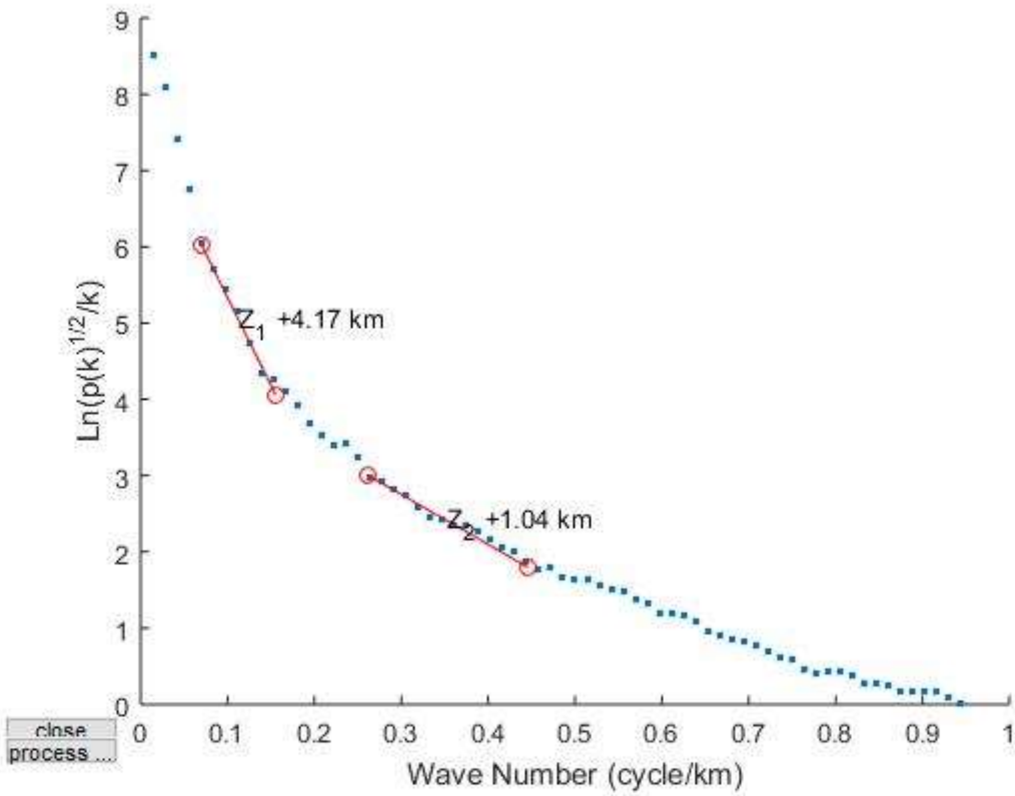

Ln(p(k)^1/2/k)
Z1 +4.17 km
Z2 +1.04 km
close
process ...
Wave Number (cycle/km)

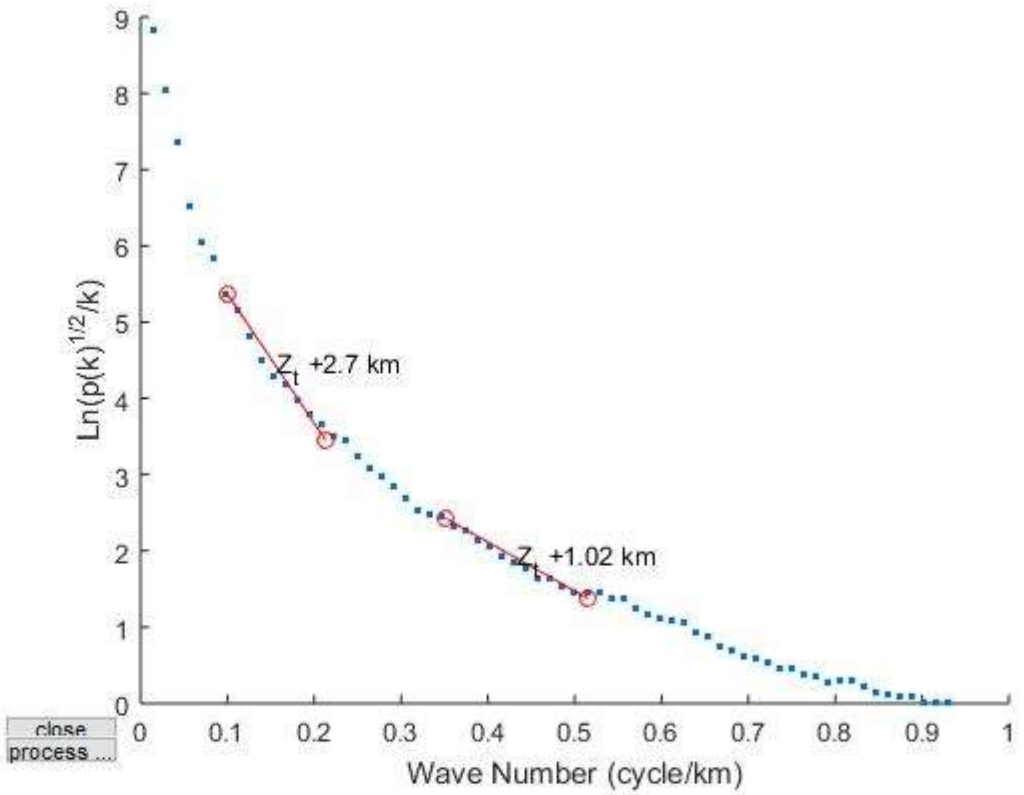

Ln(p(k)^1/2/k)
Wave Number (cycle/km)
Zt +2.7 km
Zt +1.02 km
close
process ...

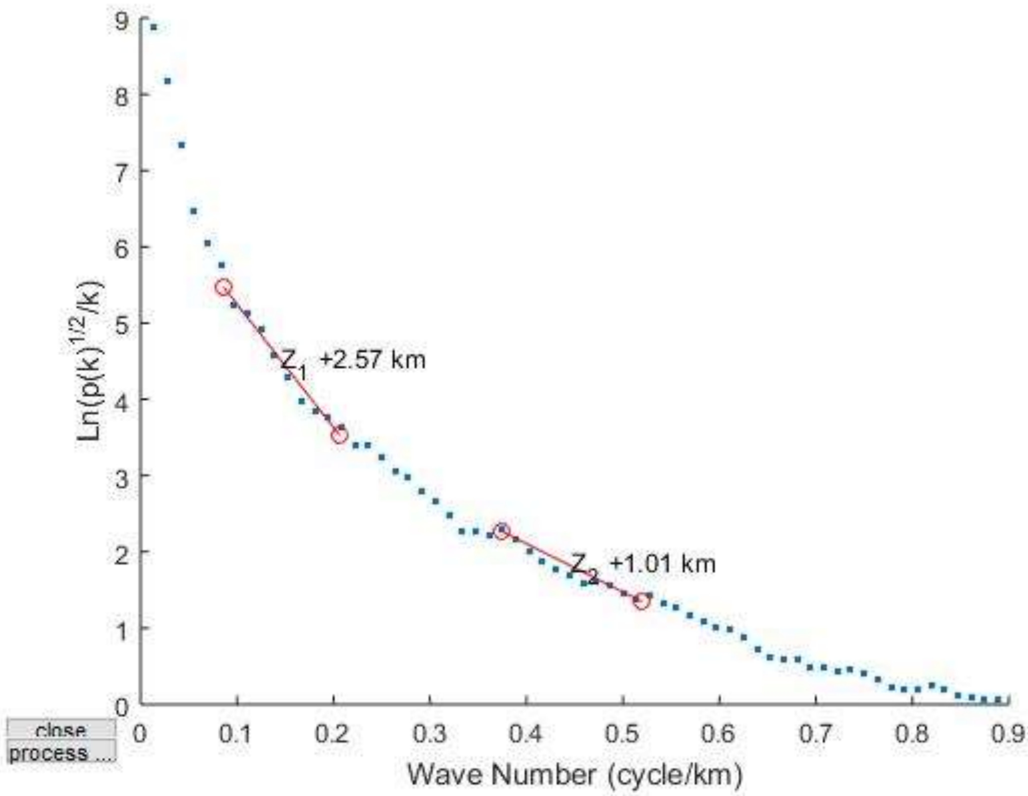

Ln(p(k)^1/2/k)
Wave Number (cycle/km)
Z1 +2.57 km
Z2 +1.01 km
close
process ...